

**THE UNIVERSITY OF TURKISH AERONAUTICAL ASSOCIATION
INSTITUTE OF SCIENCE AND TECHNOLOGY**

**MEASUREMENTS-BASED SYSTEM IDENTIFICATION OF GAS
TURBINE GENERATOR**



Master Thesis

AMEER H. SABRY

**MECHANICAL AND AERONAUTICAL ENGINEERING
DEPARTMENT**

MASTER THESIS PROGRAM

November 2017

**THE UNIVERSITY OF TURKISH AERONAUTICAL ASSOCIATION
INSTITUTE OF SCIENCE AND TECHNOLOGY**

**MEASUREMENTS-BASED SYSTEM IDENTIFICATION
OF GAS TURBINE GENERATOR**

MASTER THESIS

AMEER H. SABRY

1406080017

**MECHANICAL AND AERONAUTICAL ENGINEERING
DEPARTMENT
MASTER THESIS PROGRAM**

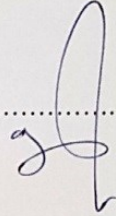
SUPERVISOR

ASSIST. PROF. DR. HABIB. GHANBARPOURASL

Ameer H. SABRY, having student number 1406080017 and enrolled in the Master Program at the Institute of Science and Technology at the University of Turkish Aeronautical Association, after meeting all of the required conditions contained In the related regulations, has successfully accomplished, in front of the jury, the presentation of the thesis prepared with the title of: "MEASUREMENTS-BASED SYSTEM IDENTIFICATION OF GAS TURBINE GENERATOR".

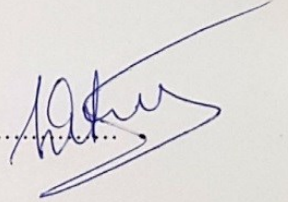
Supervisor : Assist. Prof. Dr. Habib GHANBARPOURASL

The University of Turkish Aeronautical Association



Jury Members: Assist. Prof. Dr. Yuriy ALYEKSYEYENKOV

The University of Turkish Aeronautical Association



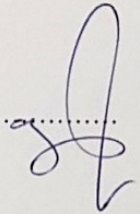
: Assist. Prof. Dr. : Kerim Youde HAN

ÇANKAYA University



: Assist. Prof. Dr. Habib GHANBARPOURASL

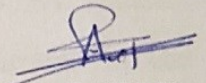
The University of Turkish Aeronautical Association



Thesis Defense Data: 30.11.2017

**THE UNIVERSITY OF TURKISH AERONAUTICAL ASSOCIATION
INSTITUTE OF SCIENCE AND TECHNOLOGY**

I hereby declare that all information in this study I presented as my Master's Thesis, called "MEASUREMENTS-BASED SYSTEM IDENTIFICATION OF GAS TURBINE GENERATOR" has been presented in accordance with academic rules and ethical conduct. I also declare and certify on my honor that I have fully cited and referenced all the sources I made used of this present study.


Ameer, SABRY

30 .11.2017

ACKNOWLEDGEMENTS

I am grateful to The Almighty GOD for helping me to complete this thesis. My Lord mercy and peace be upon our leader Mohammed peace be upon on him, who invites us to science and wisdom, and members of his family and his followers.

I would like to thank my family for supporting me throughout my academic career. Without their moral support, interest and encouragement for my academic work, the completion of this effort would not have been possible.

My ambition to obtain a master degree was fulfilled mainly because of the support and guidance I received from my advisor, Assist. Prof. Dr. Habib. GHANBARPOURASL. For his sound advice and constructive criticisms in the evaluation of the results. He has helped me at various stages during my studies and this includes providing me with a well defined thesis problem, equipping me with the necessary tools and techniques for achieving my objectives, and willingly sharing his knowledge and ideas with me. His active participation at every facet of my research work and mentoring has shaped my overall research outlook.

I would like to express my sincere gratitude to assist my brother Dr. Ahmed, for the unlimited support. His active participation at every facet of my research work and mentoring has shaped my overall research outlook

I would also like to thank Eng. Harith of AlQuds Power Plant Baghdad, for their unlimited support through and supplying a huge amount of information operation data in this work.

November 2017

Ameer H. SABRY

TABLE OF CONTENTS

ACKNOWLEDGEMENTS	iv
TABLE OF CONTENTS	v
LIST OF TABLES	vii
LIST OF FIGURES	viii
LIST OF ABBRIVIATION	xi
ABSTRACT	xii
ÖZET	xiv
CHAPTER ONE	
1. INTRODUCTION	1
1.1. Introduction	1
1.2. Literature Review	2
1.2.1. Power Plant Gas Turbine Models.....	4
1.2.2. State Space model (Levenberg–Marquardt algorithm)	5
1.2.3. Custom ANN.....	6
1.2.4. Hammerstein model	8
1.3. Problem Statement	10
1.4. Objectives	11
1.5. Scope of Work.....	11
1.6. Contributions/Novelties	12
1.7. Summary	12
CHAPTER TWO	
2. GAS TURBINE	13
2.1. Introduction	13
2.2. Gas Turbine Plants.	14
2.3. Open Cycle Single_Shaft And Twin Shaft Arrangements.....	14
2.4. Closed Cycle	16
2.5. Gas Turbine Applications.....	17
2.6. Cycles of Gas Turbine	18
2.6.1. Gas turbine cycles	19
2.6.2. Characteristics of Axial Compressor Flow	21
2.6.3. Deviation of Actual Gas-Turbine Cycles from Idealized Ones ...	23
2.6.4. Modification in The Simple Cycle.....	23
2.6.5. Gas Turbine Modeling	24
2.7. Overview on Turbine Frame 9	24

CHAPTER THREE

3. GAS TURBINE IDENTIFICATION BY ANN	29
3.1. Overview	29
3.2. Custom Neural Network.....	31
3.3. Methodology	31
3.3.1. ANN Design.....	32
3.3.2. Training algorithm.....	33
3.3.3. Deriving Model Equation.....	34
3.4. Results and Network Performance	36
3.4.1. Case 1, (3 inputs).....	36
3.4.2. Case 2, (5 inputs).....	38
3.5. Summary	44

CHAPTER FOUR

4. LINEAR AND NONLINEAR IDENTIFICATION MODELS OF GAS TURBINE	46
4.1. Introduction	46
4.1.1. Linear System Identification	47
4.1.2. Nonlinear System Identification.....	49
4.2. Transfer Function Identification.....	50
4.2.1. The fitting percentage.....	50
4.2.2. Akaike's Final Prediction Error (FPE)	50
4.2.3. Pole Zero Map	52
4.2.4. Step and Impulse Responses	53
4.3. Determining whether the system is stable.....	53
4.4. State Space	53
4.5. Estimate state-space models.....	55
4.6. Results of State Space Estimation.....	56
4.6.1. 6 th order state space model:.....	56
4.6.2. 2nd order state space model:	58
4.6.3. Impulse Responses	59
4.7. Nonlinear Approximations with Nonlinear Descriptions.....	61
4.8. Results (Nonlinear Model).....	65

CHAPTER FIVE

5. CONCLUSIONS AND RECOMMENDATION	70
5.1. CONCLUSIONS.....	70
5.2. Recommendations	71
REFERENCES	73

LIST OF TABLES

Table 1.1: A summary of noteworthy contributions for gas turbine power plant.	9
Table 2.1: Technical specification of the turbine	26
Table 4.1: Most frequent cases of partial parametric model.....	48
Table 5.1: A comparison of the models under study.	71

LIST OF FIGURES

Figure 1.1 : Introductory Diagram.....	2
Figure 2.1 : A Heat – Exchanger Might be Added.....	15
Figure 2.2 : A Heat-Exchanger Proposed of Use When The Fuel	15
Figure 2.3 : Gas turbine with separate power turbine.....	16
Figure 2.4 : Simple closed cycle gas turbine	17
Figure 2.5 : GE-9H gas turbine is prepared for testing (Source: GE Power Systems)	18
Figure 2.6 : A GE Frame 9F ready for shipping. (Source: GE Power Systems)	18
Figure 2.7 : (a) and (b).....	19
Figure 2.8 : (a) and (b).....	19
Figure 2.9 : Compressor airflow characteristics	22
Figure 2.10 : The deviation of an actual gas-turbine cycle from the ideal Brayton cycle as a result of irreversibilities.	23
Figure 2.11 : A typical free power turbine. (Source: Rolls-Royce, UK).....	25
Figure 3.1 : Flow Diagram of The Adopted ANN Methodology in System Identification.....	30
Figure 3.2 : One-Layer Network With Three Inputs, Four Neurons, and One Output neuron (Power)	33
Figure 3.3 : Training Algorithm of The Proposed Custom Neural Network.	34
Figure 3.4 : Training Process Along With Performance Index Measuring For 3 Inputs.	37
Figure 3.5 : Comparison Between Simulated and The Predicted.	38
Figure 3.6 : Training Process Along With Performance Index Measuring For 5 Inputs.	38
Figure 3.7 : Comparison Between Simulated and The Predicted.	40
Figure 3.8 : Comparison of Data Fields Measurements and Network Power (Mwatt) With Time (Sec).	41

Figure 3.9	: Error Curve of Custom ANN Model.....	41
Figure 3.10	:The Model Output Power With Respect to Each Input; (a) Fuel Consumption (FC), (b) Fuel Perce (FP), (c) Exhaust Temperature (ET), (d) Inlet Guide Vane (IGV),and (e) Compressor Air Pressure (Cp).....	44
Figure 4.1	: Sample Control System Block Diagram.....	46
Figure 4.2	: Pole-Zero Map	52
Figure 4.3	: Time Response Comparison Between The Validation/Output Power (Gen. Power) and The Model Estimated (tf3)	52
Figure 4.4	: Step and Impulse Responses	53
Figure 4.5	: System Models (System Inputs and Outputs).	54
Figure 4.6	: 6 th Order Comparison Between The State Space Model and The Measurements.....	57
Figure 4.7	: Error Curve of Linear Model	58
Figure 4.8	: 2 nd Order Model Comparison Between The State Space Model and The Measurements.....	59
Figure 4.9	: Impulse Responses Comparison for the 2nd & 6th Order Models. Each One Represents The Output Power Response Due to: (a) Exhaust Temperature, (b) Fuel percentage, (c) Fuel Consumption, (d) I G V(e). Compressor Pressure.....	61
Figure 4.10	: Open-Loop Hammerstein System With Static Memory Less Nonlinear Map F(O) and Linear Plant Model G.	62
Figure 4.11	: Block Diagram of A Hammerstein-Wiener Model.....	62
Figure 4.12	: (Ha.-w.) Output Error System.....	63
Figure 4.13	: The General Hammerstein-Wiener Model Structure, Which Consists of Sandwiching A Linear Time Invariant System\ L Between Memory Less Nonlinearities fH and fW.	65
Figure 4.14	: The General Hammerstein-Wiener Model Structure, Which Consists Of	66
Figure 4.15	: Linear, Non-Linear Models and The Field Measurements	67

Figure 4.16 : Linear, Non-linear models and the field measurements (zoom in)
..... 67

Figure 4.17 : Error Curve of Non-Linear (Hammerstein) Model..... 68

Figure 4.18 : Linear, Non-Linear, ANN Models and The Field Measurements
..... 68

Figure 4.19 : Comparison Between Error Curves Due to The Non-Linear
[Hammerstein, Ann] Model and The Linear Model..... 69



LIST OF ABBRIVIATION

GT	: Gas Turbine
P	: Power (MW)
FC	: Fuel Consumption
FP	: Fuel Percentage
ET	: Exhaust temperature
IGV	: Inlet Guide Vane
C_p	: Compressor Air Pressure
<i>tf</i>	: transfer function
ANN	: Artificial Neural Network
ARMAX	: Autoregressive Moving Average exogeneous
ARX	: Autoregressive exogeneous
NARX	: Nonlinear Autoregressive With Exogenous Inputs
SISO	: Single Input Single Output
MIMO	: Multiple-Input Multiple-Output
MISO	: Multiple-Input Single-Output
MSE	: Mean Square Error
GTPP	: Gas Turbine Power Plant
CBM	: Condition Based Maintenance
DAE	: Differential Algebraic-Equations
AVRs	: Automatic Voltage Regulators
T	: Temperature (K)
ρ	: Density of the air
W_C	: Compressor Work
W_{GT}	: Power output of ideal cycle
W_T	: Turbine expansion power
η_c	: Compressor isentropic efficiency
γ	: Specific heat ratio
η_T	: Turbine isentropic efficiency
RUL	: Remaining Useful Life
NBLM	: Neighborhood-based LM
LM	: Levenberg–Marquardt
HWM	: Hammerstein-Wiener Model

ABSTRACT

MEASUREMENTS-BASED SYSTEM IDENTIFICATION OF GAS TURBINE GENERATOR

SABRY, Ameer

M.Sc., Mechanical Engineering Department

Supervisor: Assist. Prof. Dr. Habib GHANBARPOURASL

November 2017, 78 pages

The employing of gas turbines has grown rapidly in electrical energy production following the economic growth and increased demand for electricity. Modelling and control of gas turbines (GTs) have always been a controversial issue because of the complex dynamics of these kinds of equipment. Considerable research activities have been carried out so far in this field in order to disclose the secrets behind the nonlinear behaviour of those systems. Although the results of the research in this area have been satisfactory so far, it seems that there is no end to the efforts for performance optimization of gas turbines. A variety of analytical and experimental models as well as control systems have been built in the prior art for gas turbines. However, the need for optimized models for different objectives and applications has been a strong motivation for researchers to continue to work in this field. Since the problems of gas turbine such as; internal faults, and the load fluctuations on the power distribution network may cause grid instability issues, it is essential to consider accurate dynamic modelling of gas turbine system. In this research, several approaches for system identification are implemented to characterize the dynamic behavior of the gas turbine system for the purposes of monitoring, diagnostics, parameter estimation and control design. The assessment of the applied method evaluated by the fitting percentage to estimate the experimental data and the Mean Square Error (MSE).

The challenges faced when a practical field measurements have been adopted for the gas turbine model GE Frame 9E of the Alquds-Iraq power plant as a multi-input case study. Firstly, data analysis has been applied to classify the input-input and input-output relationships for reducing the number of inputs. Initially, a linear model with the most effective parameters represented by the Fuel Consumption (FC) and Exhaust Temperature (ET), has been evaluated for the measurements of the system to attain some preliminary insight into the data characteristics. Then, a nonlinear least squares with automatically chosen line search has been carried out, we started by evaluating a default-order discrete model which assumes 2 poles and 1 zero for each transfer function. The input/ output delay and the sampling time have been extracted from the real measurements of the field data. Hammerstein model is proposed with new iterative gradient descent as a prediction and error minimization method to identify the dynamic model of the gas turbine and to parameterize the nonlinear mapping. Finally, a modification to existing custom feed forward neural network has been implemented to extract another modelling mathematical equation with the number of neurons equal to the number of inputs to simplify the solution of the resultant modelling equation. A comparative table of suitable evaluation parameters has been presented to conclude the findings of the work. The identification methods are formulated to permit their application and to provide a procedure for further future application and modifications.

Keywords: Gas Turbines, System Identification, Dynamic Model, Mathematical Equation.

ÖZET

GAZ TÜRBİN JENERATÖRÜNÜN ÖLÇÜMLER DAYALI SİSTEM TANI

SABRY, Ameer

Yüksek Lisans, Makine Mühendisliği Bölümü

Danışman: Yrd. Doç. Dr. Habib GHANBARPOURASL

Kasım 2017, 78 sayfa

Ekonomik büyümeyi takiben elektrik enerjisi üretiminde ve elektrik talebinde artış nedeniyle gaz türbinlerinin istihdamı hızla büyümüşür. Gaz türbinlerinin (GT) modellenmesi ve kontrolü, bu tür ekipmanların karmaşık dinamikleri nedeniyle her zaman tartışmalı bir konu olmuştur. Bu sistemlerin doğrusal olmayan davranışının arkasındaki sırları açığa çıkarmak için bugüne kadar önemli araştırma faaliyetleri yapılmıştır. Bu alandaki araştırmanın sonuçları bugüne kadar tatmin edici olmakla birlikte, gaz türbinlerinin performans optimizasyonu için çabaların sona ermediği görülmektedir. Önceki teknolojide gaz türbinleri için çeşitli analitik ve deneysel modellerin yanı sıra kontrol sistemleri yapılmıştır. Bununla birlikte, farklı hedefler ve uygulamalar için optimize edilmiş modellere duyulan ihtiyaç, araştırmacıların bu alandaki çalışmalarına devam etmeleri için güçlü bir motivasyondur. Gaz türbini gibi problemler yüzünden; dahili arızalar ve güç dağıtım şebekesindeki yük dalgalanmaları ızgara istikrarsızlığı sorunlarına neden olabilir. Gaz türbini sisteminin doğru dinamik modellemesini dikkate almak esastır. Bu çalışmada, izleme, teşhis, parametre tahmini ve kontrol tasarımı için gaz türbini sisteminin dinamik davranışını karakterize etmek için ve sistem tanımlama için çeşitli yaklaşımlar uygulanmaktadır. Uygulanan yöntemin deney verilerinin tahmin edilmesinde, uyma yüzdesi ile değerlendirilmesi

ve Ortalama Kare Hata (MSE) değerlendirilmesidir. Alquds-Irak elektrik santralının GE Frame 9E gaz türbini modeli için çok girişli bir vaka çalışması olarak pratik bir saha ölçümleri yapıldığında karşılaşılan zorluklardır. İlk olarak, girdi sayısını azaltmak için girdi-girdi ve girdi-çıkı ilişkilerini sınıflandırmak için veri analizi uygulanmıştır. Başlangıçta, Yakıt Tüketimi (FC) ve Egzoz Sıcaklığı (ET) ile temsil edilen en etkili parametrelere sahip doğrusal bir model, sistemin ölçümleri için veri özelliklerine ilişkin ön öngörü elde etmek için değerlendirildi. Daha sonra otomatik olarak seçilen hat aramasında doğrusal olmayan en küçük kareler gerçekleştirildi. Her aktarım fonksiyonu için 2 kutup ve 1 sıfır varsayarak, varsayılan emir ayrık bir model değerlendirerek başlandı. Giriş / çıkış gecikmesi ve örnekleme zamanı alan verilerinin gerçek ölçümlerinden çıkarılmıştır. Hammerstein modeli, gaz türbininin dinamik modelini tanımlamak ve doğrusal haritalama parametrelerini belirlemek için bir tahmin ve hata minimizasyon yöntemi olarak yeni iterasyon gradyen inişiyile önerilmiştir. Sonuç olarak elde edilen modelleme denkleminin çözümünü basitleştirmek için ve giriş sayısına eşit sayıda nöron bulunan başka bir modelleme matematiksel denklemi çıkarmak için, mevcut özel ileriye beslemeli sinir ağı üzerinde bir değişiklik yapılmıştır. Çalışmanın bulgularını tamamlamak için uygun değerlendirme parametrelerinin karşılaştırmalı bir tablosu sunulmuştur. Belirleme yöntemleri, başvurularına izin vermek ve daha ileri uygulama ve tadilatlar için bir prosedür sağlamak üzere formüle edilmiştir.

Anahtar kelimeler: Gaz Türbinleri, Sistem Tanımlama, Dinamik Model, Matematik Denklem.

CHAPTER ONE

INTRODUCTION

1.1. Introduction

The accurate modelling of power plant systems, excitation systems and prime movers to predict power station performance is clearly a very important topic that has been the subject of interest for several decades. In the history of energy conversion, the gas turbine is a relatively new energy converter. Nowadays, gas turbines, which run on natural gas, diesel fuel, biomass gases and. etc, are a natural power plant for offshore platforms because of their compactness, low weight, and multiple fuel applications. Therefore, the gas turbine has found increasing service in the power industry. Since gas turbine internal faults or distribution network load fluctuations may cause instabilities in the grid, it is necessary to investigate an accurate dynamical model for a gas turbine system. The chapter is organized as follows: Section 1.1 Measurements-Based System Identification of Gas Turbine Generator. Section 1.2 Literature Review. Section 1.3 Problem Statement 1.4. Scope of Work 1.5 Novelties, the details can be seen in Figure 1.1.

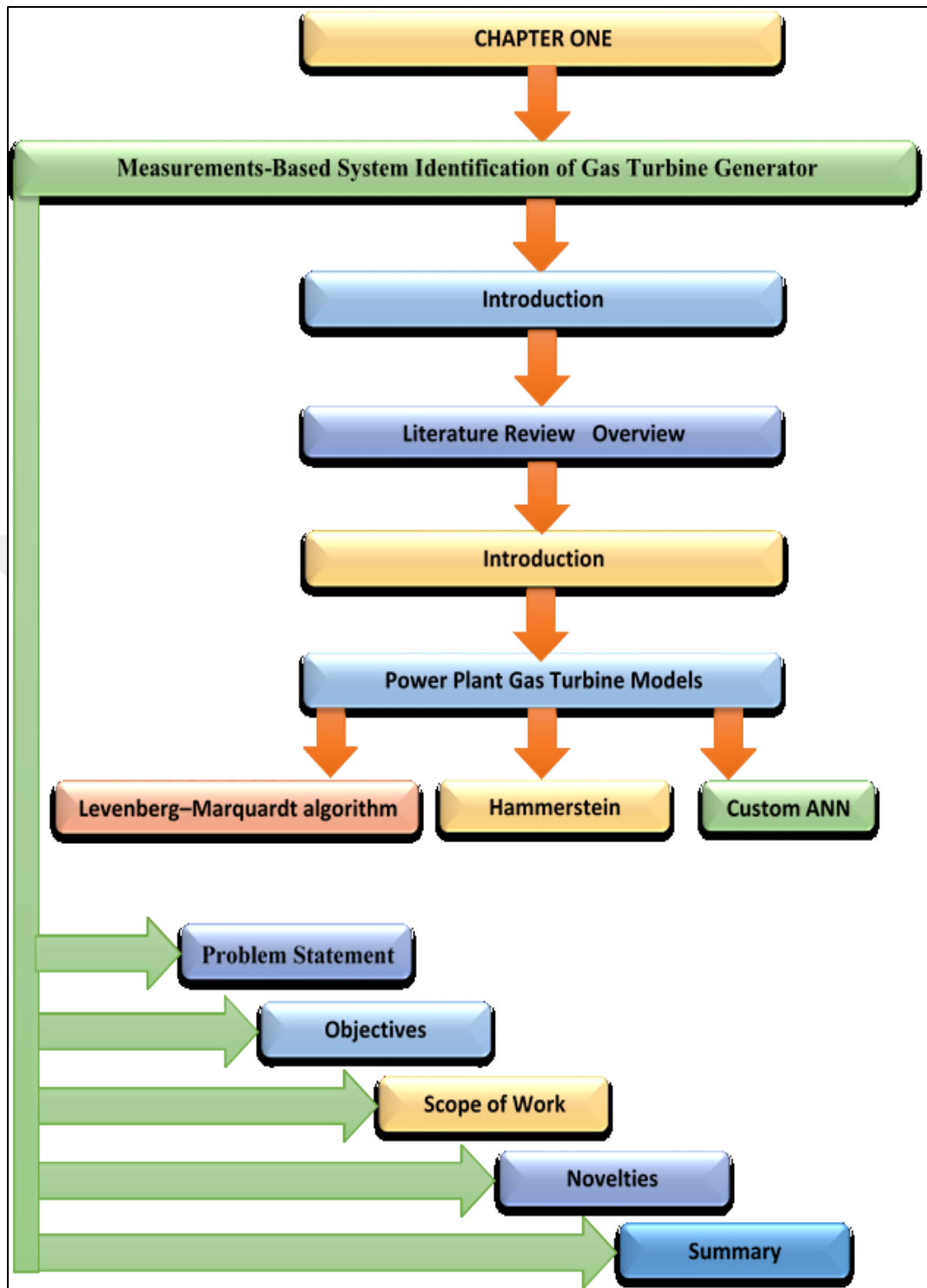


Figure 1.1: Introductory Diagram

1.2. Literature Review

Modelling and control of gas turbines (GTs) have always been a controversial issue because of the complex dynamics of these kinds of equipment. Considerable research activities have been carried out so far in this field in order to disclose the

secrets behind the nonlinear behaviour of these systems. Although the results of the research in this area have been satisfactory so far, it seems that there is no end to the efforts for performance optimization of gas turbines. A variety of analytical and experimental models as well as control systems have been built so far for gas turbines. However, the need for optimized models for different objectives and applications has been a strong motivation for researchers to continue to work in this field. The work in this chapter is aimed at presenting a general overview of essential basic criteria that need to be considered for making a satisfactory model and control system of a gas turbine. GT type, GT configuration, modelling methods, modelling objectives as well as control system type and configuration are the main preliminary factors for modelling a gas turbine which will be briefly discussed in the chapter. Some of the research in this field will also be stated shortly.

Critical engineering systems, such as gas turbines, require dynamic maintenance planning strategies and predictions in order to reduce unnecessary maintenance tasks. A condition based maintenance (CBM) decision-making strategy based on the observation of historical condition measurements can make predictions for the future health conditions of systems and this capability of predictions makes CBM desirable for the systems reliability, maintenance, and overall operating costs [1]. The predictions on the health level of the system can be provided to maintenance scheduling and planning. This is especially useful in demanding applications, where the maintenance must be performed safely and economically for an entire lifetime.

Prognostics can be defined as the process of predicting the lifetime point at which a component or a system could not complete the proposed function planned during its design [2]. The amount of time from the current time to the point of a system's failure is known as Remaining Useful Life (RUL)[3]. The concept of RUL has been widely applied as a competitive strategy to improve maintenance planning, operational performance, spare parts provision, profitability, reuse and product recycle [4]. The prediction of RUL is the principal goal of machine prognostics and this paper, therefore, evaluates the prognostics as the calculation of RUL for turbofan engine systems.

Data-driven prognostics are more effective methods in gas turbine prognostic applications because of the simplicity in data and consistency in complex processes [5].

1.2.1. Power Plant Gas Turbine Models

A single-shaft gas turbine design and off-design model was presented by Lazzaretto and Toffolo [6]. They used analytical method and feedforward neural network as two different approaches to model the system. Appropriate scaling techniques were employed to construct new maps for the gas turbine using the available generalized GT maps. The new maps were validated using the obtained experimental data. Ogaji et al. applied three different architectures of artificial neural networks (ANNs) for multi-sensor fault diagnosis of a stationary twin-shaft gas turbine using neural network [7]. The results indicated that ANNs could be used as a high-speed powerful tool for real-time control problems. Arriagata et al. applied ANNs for fault diagnosis of a single-shaft industrial gas turbine [8]. They obtained a comprehensive data set from ten faulty and one healthy engine conditions. The data were trained using feedforward multi-layer perceptron (MLP) structure. The results proved that ANNs could identify the faults and generate warnings at early stages with high reliability. Basso, Giarre, Groppi and Zappa applied a nonlinear autoregressive with exogenous inputs (NARX) model to identify dynamics of a small heavy-duty power plant gas turbine [9]. The objective was to make an accurate reduced-order nonlinear model using black-box identification techniques. They considered two operational modes for the gas turbine; when it was isolated from power network as a stand-alone unit and when it was connected to the power grid. They showed that in order to reduce the complexity and improve the simulating capability of the model, the ingredients should be chosen carefully. Bettocchi et al. investigated artificial neural network model of a single-shaft gas turbine as an alternative to physical models [10]. They observed that ANNs can be very useful for the real time simulation of GTs especially when there was insufficient information on the system dynamics and behaviour. In another effort, Bettocchi et al. developed a multiple-input and multiple output (MIMO) neural network approach for diagnosis of single-shaft gas turbine engines [11]. A NARX model was applied to model a power plant micro gas turbine (MGT) and the related distribution system dynamics by Jurado [12]. However, the nonlinear terms in the model were restricted to second order. The resulted model was capable of modelling both low and high amplitude dynamics of MGTs. The quality of the model was examined by cross validation technique. The model was tested under different operational conditions and electrical disturbances. Geon applied ANN to

prognosticate key parameters in turbine hall and to identify GT key cost drivers [13]. The study just focused on the construction of turbine hall section. The results of the research showed that the ANN regression model was reliable and could be used by the contractors to estimate turbine hall construction process. Spina and Venturini applied ANN to train operational data through different patterns in order to model and simulate a single-shaft gas turbine and its diagnostic system with a low computational and time effort [14]. Magnus Fast et al. applied simulation data and ANN to examine condition-based maintenance of gas turbines [15]. In another effort, Fast et al. used real data obtained from an industrial single-shaft gas turbine working under full load to develop a simple ANN model of the system with very high prediction accuracy [16]. A combination of ANN method and cumulative sum (CUSMUS) technique was utilised by Fast et al. for condition monitoring and detection of anomalies in GT performance [15]. To minimise the need for calibration of sensors and to decrease the percentage of shut-downs due to sensor failure, an ANN-based methodology was developed for sensor validation in gas turbines by Fast et al. [17]. Application of ANN to diagnosis and condition monitoring of a combined heat and power plant was discussed by Fast et al. [18]. Fast applied different ANN approaches for gas turbine condition monitoring, sensor validation and diagnosis [19]. Yoru et al. examined application of ANN method to exergetic analysis of gas turbines which supplied both heat and power in a cogeneration system of a factory [20]. They compared the results of the ANN method with the exergy values from exergy analysis and showed that much closer exergetic results could be attained by using ANN method. Application of ANNs and ANFIS to micro gas turbines was investigated by Bartolini et al.[21]. They investigated the effects of changes of ambient conditions (temperature, pressure, humidity) and load on MGTs output power. The results indicated that ambient temperature variations had more effect on the output power than humidity and pressure. Besides, MGTs were less influenced by ambient conditions than load.

1.2.2. State Space model (Levenberg–Marquardt algorithm)

All these algorithms can be considered as variations of the steepest descent method, because they only use information of the objective function and its gradient. It is possible, however, to estimate the Hessian matrix of the error function by using only the values of the first derivatives of the networks outputs with respect to the

weights and, with this information, obtain better values for the variation of the network weights at each learning cycle. This is one of the observations that led to the development of the Levenberg–Marquardt (LM) method [22]&[23]. The LM algorithm, taken from the optimization field, has increased its popularity within the neural networks community in the last few years. The difference between optimization and neural-network applications of the method comes from the fact that in the latter there are often many parameters that need to be estimated.

Although the results achieved with this method are very good, its application to neural networks suffers from some drawbacks, derived from its nonlocal nature (the changes in the weights of a neuron depend on the errors due to far neurons).

- It is not biologically feasible.

- It is both time and memory consuming. The first problem is due to the fact that biological neurons only have information about what is happening in some neighborhood. We have recently [24] developed the neighborhood-based LM (NBLM) method that, through the use of the neural neighborhood concept, improves the behavior of the LM algorithm in both time and memory concerns. In that work, the feasibility of the method was proved and some preliminary tests were carried out. However, as the software used for the simulations was an adaptation of the LM routine included in Neural Network, which only takes into account successful cycles, it was not easy to quantify the training time, which is essential to compare the performance of the method with other widely used algorithms. So our main goal in this work was to implement the method using routines based on those found in LINPACK[25].

1.2.3. Custom ANN

There are particular importance because of the ability to integrate innovative and conventional approaches by generating inclusive prognostic methods over a wide-ranging data series. The most commonly practiced data-driven prognostic methods in the literature are the Artificial Neural Networks (ANNs) [26] & [5]. ANNs are computational algorithms inspired by biological neural networks of the brain and are used as machine-learning systems made up of data processing neurons, which are the units to connect through computation of output value by the input data. They learn by example by identifying the unique output with many past inputs values [27]. Neural networks are effective applications to model engineering tasks consisting of a broad

category of nonlinear dynamical systems, data reduction models, nonlinear regression and

discriminant models [28]. In some complex engineering applications, the observations from the system may not include precise data, and the desired results may not have a direct link with the input values. In such cases, ANN is a powerful tool to model the system without knowing the exact relationship between input and output data [29]. In particular, when a longer horizon with several steps ahead long term predictions is required, the recurrent neural networks play an important role in the dynamic modelling task by behaving as an autonomous system, and endeavouring to recursively simulate the dynamic behaviour that caused the nonlinear time series [30]; [31]; [32]. Recurrent Neural Network structure applies the target values as a feedback into the input regressor for a fixed number of time steps [33]. Multi-step long term predictions with dynamic modelling are suitable for complex system prognostic algorithms since they are faster and easy to calculate compared to various other prognostics methods. The recurrent neural networks, therefore, have been widely employed as one of the most popular data-driven prognostics methods and a significant number of studies across different disciplines have stated the merits of them by introducing different methodologies. However, ANN multi-step predictions in prognostic applications can be quite challenging when only a few time series or a little previous knowledge about the degradation process is available and the failure point is expected to happen in the longer term. The greater interest in neural networks is the accomplishment of learning but it is not always possible to train the network as desired. The results at multi-step long-term time series predictions may be ineffective and this is generally more evident in the time series having exponential growths or decays. In this paper, a Nonlinear Auto Regressive neural network with Exogenous inputs (NARX) is designed to make future steps of predictions for an engine from past operational values. The model learns successfully to make predictions of time series that consists of performance related parameters. The designed prognostic method is modeled by using turbofan engine simulation C-MAPSS data sets from NASA data repository [34]. The results demonstrate the relationship between the historical performance deterioration of an initially trained subset and the RUL prediction of a second test subset.

1.2.4. Hammerstein model

The Hammerstein model is a special kind of nonlinear systems which has applications in many engineering problems and therefore, identification of Hammerstein models has been an active research topic for a long time. Existing methods in the literature can be roughly divided into six categories: the iterative method, the over-parameterization method, the stochastic method, the nonlinear least squares method, the separable least squares method, and the blind method [35]. Frequency domain identification methods for a linear system are well understood and developed [36]. This idea will be used to Hammerstein models. By exploring the fundamental frequency, the linear part and the nonlinear part can be identified.

A thorough introduction to the gas turbine theory is provided in [37]. There exist a large number of publications on the modeling of gas turbines. The model complexity varies according to the intended application. A detailed first principle modeling based upon fundamental mass, momentum and energy balances is reported by [38] and [39]. These models describe the spatially distributed nature of the gas flow dynamics by dividing the gas turbine into a number of sections. Throughout each section, the thermodynamic state is assumed to be constant with respect to location, but varying with respect to time. Mathematically, the full partial differential equation model is reduced to a set of ordinary differential equations, which are facilitated easily within a computer simulation program. For a detailed model, a section might consist of a single compressor or turbine stage. Much simpler models result if the gas turbine is decomposed into just three sections corresponding to the main turbine components, i.e. compressor, combustor and turbine, as in [40]. Instead of applying the fundamental conservation equations, as described above, another modeling approach is to characterize the gas turbine performance by utilizing the real steady state engine performance data, as in [41]. It is assumed that transient thermodynamic and flow processes are characterized by a continuous progression along the steady state performance curves, which is known as the quasi-static assumption. The dynamics of the gas turbine, e.g. combustion delay, motor inertia, fuel pump lag etc. are then represented as lumped quantities separate from the steady-state performance curves. Very simple models result if it is further assumed that the gas turbine is operated at all times close to the rated speed [42].

Table 1.1. Presents a summary of noteworthy contributions of models estimated for gas turbine power plant.

Table 1.1: A Summary of Noteworthy Contributions For Gas Turbine Power Plant.

Reference	System Type	Method	Results/Conclusions
[43]	Nonlinear system	ANN(Artificial Neural Network) identification techniques are developed to estimate a General Electric Frame 9, 116MW	Electrical power and exhaust gas temperature are chosen as system main outputs which can be expressed by fuel flow, shaft speed and compressor inlet guide vanes considering the ambient temperature effects. The operating condition of the gas turbine during identification procedure is considered from full speed no load to full load.
[44]	nonlinear	One method for estimating this stress situation is to utilize a database.	The nonlinear, dynamic behavior of the subject engine is calculated solving a number of systems of partial differential equations, which describe the unsteady behaviour of each component individually. To identify each differential equation system unambiguously,
[45]	Linear models	Linear models estimated on small-signal data are first examined and the need for a global nonlinear model is established	Periodic test signals, frequency domain analysis and identification techniques, and time-domain NARMAX modeling can be effectively combined to enhance the modeling of a gas turbine.

Reference	System Type	Method	Results/Conclusions
[46]	State-space	A State-Space model is used for identification and some observer-based methods are used for residual generation, while for residual evaluation a neural network classifier for MLP is used	The proposed fault detection and isolation tool has been tested on a single-shaft industrial gas turbine simulator.
[47]	Simple mathematical	These simple mathematical expressions arise from the balance of energy flow across engine components	The parameter fit of the model to a specific engine such as the GE LM2500 detailed in this work utilizes constants and empirical fits of power conversion efficiencies obtained using data collected from a high-fidelity engine simulator such as the Gas Turbine Simulation Program (GSP).
[48]	Nonlinear	The gas-turbine model is validated by direct comparison of the model predictions with the output parameters of a commercial turbine	The influence of the pressure and temperature ratios on the overall plant efficiency and the fuel conversion rate is discussed. This kind of thermodynamic analysis is necessary in order to design efficient as well as commercially interesting new generations of plants of this type.

1.3. Problem Statement

The global gas turbine has been growing recently, Increasing awareness regarding sustainable energy sources that have shifted the industry focus towards large-scale incorporation of natural gas as a fuel for employing of gas turbines in electrical energy production following the economic growth and increased demand for electricity. Gas turbines have a very expensive, complex, and precise components functioning at high temperature and pressure of gas conditions. Performance drooping or the failure due to ambient temperature, load, or fuel delivery variations of the turbine engine will highly affect its operation. Since the problems of gas turbine such as; internal faults, and the load fluctuations on the power distribution network may cause

grid instability issues, it is essential to consider accurate dynamic modelling of gas turbine system.

1.4. Objectives

To study several approaches for system identification that could be implemented to characterize the dynamic behavior of the gas turbine system for the purposes of monitoring, diagnostics, parameter estimation and control design.

To identify the unknown nonlinear map factors, and the linear dynamics of the turbine system measurements.

To evaluate the applied modelling method by the fitting percentage to estimate the field observations, and also by the Mean Square Error (MSE).

To analyse the acquired data of the gas turbine to identify the input-input and input-output relationships in order to reduce the number of inputs and the model complexity.

To prepare the findings of this research towards a control relevant model of the existing system which facilitates the control design and improves the disturbing effects on the turbine output shaft power.

1.5. Scope of Work

The work initially, addresses a linear model with the most effective parameters represented by the fuel consumption (FC) and exhaust temperature (ET), and then evaluated with the field measurements of the system to attain some preliminary insight into the data characteristics. Later, a Nonlinear Least Squares with automatically chosen line search carried out in the same concern. The input/ output delay and the sampling time have been extracted from the real measurements of the field data. Hammerstein model is proposed with new iterative gradient descent as a prediction and error minimization method to identify the dynamic model of the gas turbine and to parameterize the nonlinear mapping. Finally, a modification to existing custom feed forward neural network has been implemented to extract another modelling mathematical equation with the number of neurons equal to the number of inputs to simplify the solution of the resultant modelling equation.

1.6. Contributions/Novelties

Intensive parametric analysis of the gas turbine type GE Frame 9E and its performance through real measurements that conducted in Alquds-Iraq power plant as a multi-input case study.

Deriving a mathematical modelling equation from the proposed custom ANN for the output power of the system as a function of measured input parameters.

Presenting a linear and non-linear modelling system to simulate and estimate the system performance according the several inputs that affect on the system output behaviour.

1.7. Summary

There are different approaches and methodologies in modelling and control of gas turbines. Choosing the right method and creating the right model based on the required application depends on different factors. In this chapter of this work, a brief overview of basic consideration for making a satisfactory model of gas turbines was discussed. A short description of each of these models and factors, including GT type, GT configuration, modelling methods, modelling objectives as well as control system type and configuration were provided. Samples of significant research related to each of the areas were presented. By highlighting the mentioned factors, remarkable enhancements can be achieved in the process of modelling and control of gas turbines.

CHAPTER TWO

GAS TURBINE

2.1. Introduction

Of the various means of producing mechanical power, the turbine is in many respects the most satisfactory. The absence of reciprocating and rubbing members means that balancing problems are few, that the lubricating oil consumption is exceptionally low, and that reliability can be high. The inherent advantages of the turbine were first realized using water as the working fluid, and hydro-electric power is still significant contributor to the world's energy resources. Around the turn of the twentieth century the steam turbine began its career and, quite apart from its wide use as marine power plant, it has become the most important prime mover for electricity generation. Steam turbine plant producing up to (500) MW of shaft power with an efficiency of nearly (40 percent) are now being used. In spite of its successful development, the steam turbine does have an inherent disadvantage [49].

It is that the production of high_ pressure high temp. Steam involves the installation of bulky and expensive steam generation equipment, whether it be a conventional, boiler or nuclear reactor. The significant feature is that the hot gases produced in the boiler furnace or reactor core never reach the turbine; they are merely used indirectly to produce an intermediate fluid, namely steam. Clearly a much more compact power plant results when the water to steam step is eliminated and the hot gases themselves are used to drive the turbine.

There are two main factors affecting the performance of gas turbine component efficiencies and turbine working temperature. The higher they can be made, the better the all-round performance of the plant. It was, in fact, low efficiencies and poor turbine materials which brought about the failure of a number of early attempts to construct a gas turbine engine. For example, in 1904 two French engineers,

Armengaud and Lemale, built a unit which did little more than turn itself over: the compressor efficiency was probably no more than 60 %, and the max. Gas temp. That could be used was about 740k. The development of the gas turbine has kept pace with the progress on aerodynamic science and metallurgy, so that it is now possible to find highly advanced engines that use a compression ratio up to 35:1, with an efficiency of the individual components a round 85 – 90 and a turbine inlet temperature up to 1650 c°.

2.2. Gas Turbine Plants.

A gas turbine plants as shown in figure. (2.1) consist of a turbo compressor, combustion chamber (or H.E) and turbine. The plant is started by rotating the compressor- turbine assembly of a starting motor arrange another device. When the compressor develops enough pressure to support combustion of the fuel in the combustion chamber, the hot gases can themselves drive the gas turbine, and the plant becomes self- steaming. The turbine should develop enough power to be able to drive the compressor and load. The output of the plant is the difference between the turbine work and the compressor work. The actual output at the generator terminals will be much less than this. Gas turbine plants can be compared with steam turbine plants; the chief distinguishing features of the gas turbine plants are their high melt gas temp. ($t_{max} >1500k$) and lower pressure. The exhaust gas pres. of the gas turbine plants are nowhere near the considerably low pressure. (22.5mbar) employed in the condensing steam plants. This explains why it is not necessary to employ large low pressure. cylinders and multiple exhaust even large terrestrial gas turbine plant [50].

2.3. Open Cycle Single_Shaft And Twin Shaft Arrangements

If the gas turbine is required to operate at a fixed speed and fixed load condition such as in peak load power generation schemes, the single – shaft arrangement shown in Figure 2.1 may be suitable. Flexibility of operation, i.e. the rapidity with which machine can accommodate itself to changes of load and rotational speed, and efficiency at part lad, are in this case an important. Indeed, the effectively high inertia due to the drag of the compressor is an advantage because it reduces the danger of cover speeding in the event of a loss of electrical load. A heat – exchanger might be added as in Figure 2.1 to improve the thermal efficiency, although for a given size of

plant, the power plant output could be reduced by as much as 10 % due to frictional losses. Losses in the heat - exchanger.

Figure 2.2 shows modified from proposed of use when the fuel, e.g. pulverized coal, is such that the products of combustion contain constituents which corrode or erode the turbine blades. It is much less efficient than the normal cycle because the heat - exchanger, inevitably less than perfect, is transferring the whole of the energy input instead of merely a small part of the it. Such a cycle would only be considered if a supply of 'dirty' fuel was available at very low cost [51].

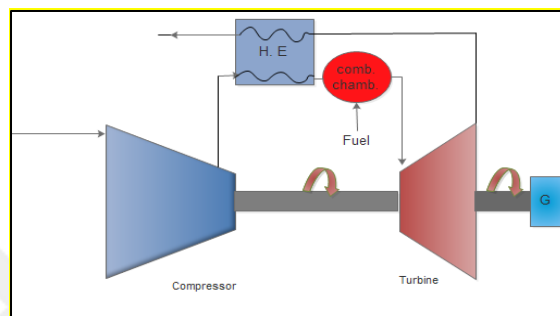


Figure 2.1: A Heat - Exchanger Might be Added

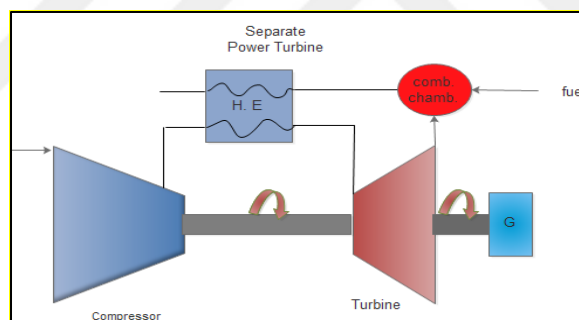


Figure 2.2: A Heat-Exchanger Proposed of Use When The Fuel

When flexibility in operation is of paramount importance, such as in road, rail and marine application, the use of mechanically independent (or free) power turbine is desirable. This twin - shaft arrangement Figure 2.3 the high - pressure turbine drives the compressor and the combination acts as a gas generator for the low - pressure power turbine.

Twin shaft arrangement is also used for large scale electricity generation units, with the power turbine designed to run at the alternator speed without the need for an expensive reduction gear box. A minor advantage is that the starter unit need only be sized to turn over the gas generator. A disadvantage, however, is that a shedding of

electrical load can lead to rapid over – speeding of the power turbine, and the control system must be designed to prevent this [52].

Notice: For any given compressor Pres. Ratio the power required per unit quantity of working fluid is directly proportional to the inlet temp.

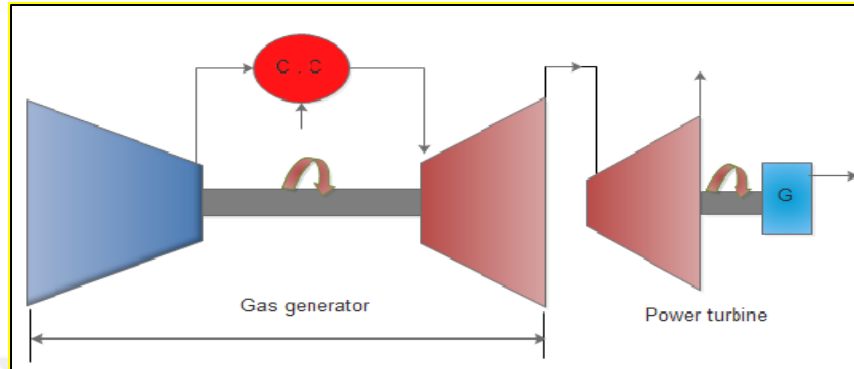


Figure 2.3: Gas Turbine With Separate Power Turbine

2.4. Closed Cycle

Outstanding among the many advantages claimed for the closed cycle is the possibility of using a high pressure (and hence a high gas density) throughout the cycle, which would result in a reduced size of turbo machinery for a given output and enable the power output to be altered by a change of pressure level in the circuit, this form of control means that a wide range of load can be accommodated without alteration of the max. cycle temperature and hence with little variation of overall efficiency. The chief disadvantages of the closed cycle is the need for an external heating system, which involves the use of an auxiliary cycle and introduces a temperature difference between the combustion gases and the working fluid. The allowable working temperature of the surfaces in the heater will therefore impose an upper limit on the maximum temperature of the main cycle [53]. A typical arrangement of a closed cycle gas turbine is shown in Figure 2.4. The cycle includes a water-cooled pre-cooler for the main cycle fluid between the heat-exchanger and compressor. In this particular arrangement, the gas heater forms part of the cycle of an auxiliary gas turbine set, and power is controlled by means of a blow-off valve and an auxiliary supply of compressor gas as shown. The high density of the working fluid improves heat transfer, so that more effective heat-exchanger is possible. At the time of writing dozen or so closed cycle plants of (2 – 20 MW) output have been built, mostly from the Escher – Ways stable, and all with air as the working fluid but burning various fuels

such as coal, natural gas, blast furnaces gas and oil. Turbine inlet pressure at up to forty atmospheres have been used. With helium, larger sets of up to (250 MW) are thought to be possible.

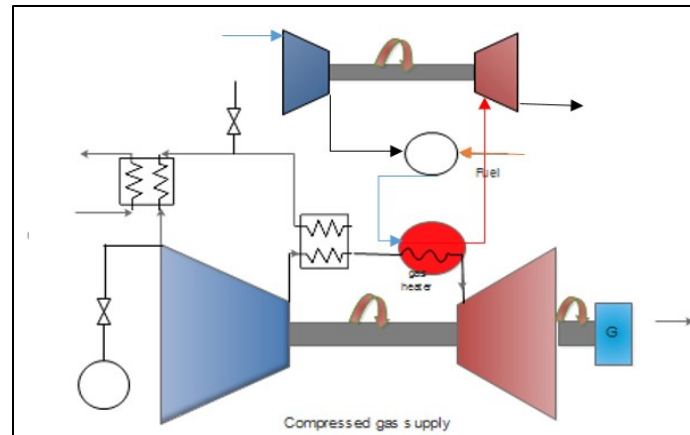


Figure 2.4: Simple Closed Cycle Gas Turbine

2.5. Gas Turbine Applications

Sometimes we shall find it necessary to use the distinguishing terms 'aircraft gas turbine and "industrial gas turbine ". The first term is self-explanatory, while the second is intended to include all gas turbines not included in the first category. This broad distinction has to be made for three main reasons: Firstly, the life required of an industrial plant is of the order of (100000 hours) without major over haul, whereas this is not expected of an aircraft gas turbine. Secondly, limitation of the size and weight of an aircraft power plant is much more important than in the case of most other application. Thirdly, the aircraft power plant can make use of the kinetic energy of the gases leaving the turbine, whereas it is wasted in other types and consequently must be kept as low as possible.

Finally, the gas turbine can be used as a compact air compressor suitable for supplying large quantities of air at moderate pressure. In this case the turbine produced just sufficient power to drive the compressor and the net power output is in the form of compressed air bled from the compressor. Figure 2.5 and Figure 2.6 show an industrial gas turbine during assembly at the OEM's facility.

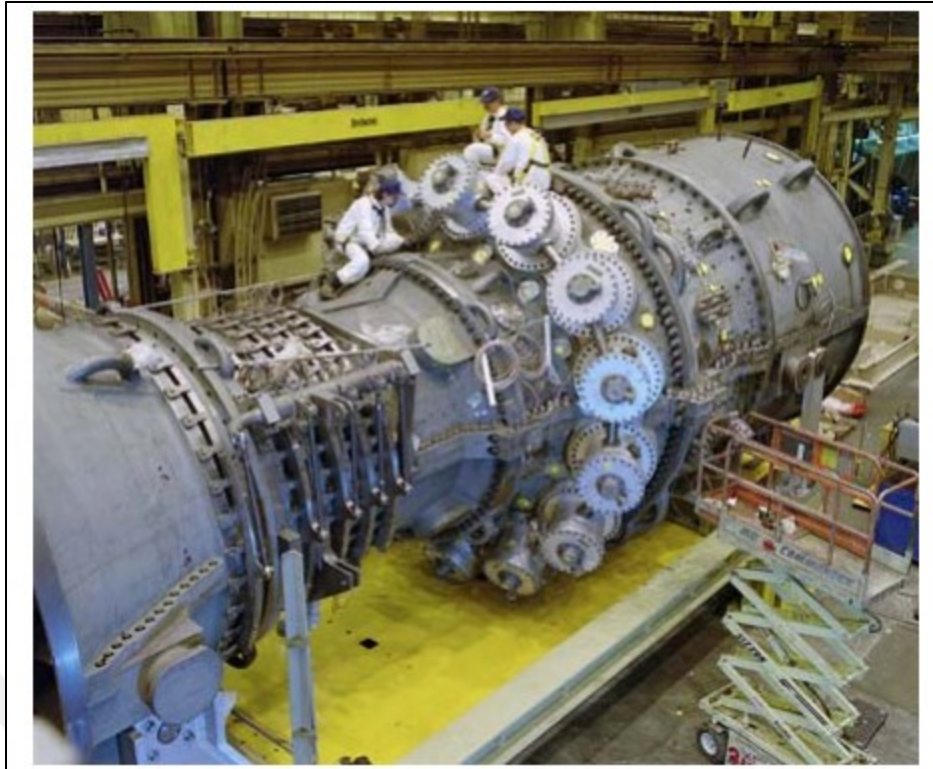


Figure 2.5: GE-9H gas turbine is prepared for testing (Source: GE Power Systems)



Figure 2.6: A GE Frame 9F ready for shipping. (Source: GE Power Systems)

2.6. Cycles of Gas Turbine

Gas turbine cycles are classified according to the type of fuel combustions that taking place inside the combustion chamber i. Constant pressure cycle, known as the Joule or Brayton cycle (The Brayton cycle is an idealization of a simple gas turbine proposed by Brayton in the 1870's It is a 4 step cycle), as shown in Figure 2.7 (a) and

(b) and Figure 2.8 (a) and (b). If the combustion in the chamber take place at constant pressure and letting the volume to increase, then it is called the constant pressure cycle

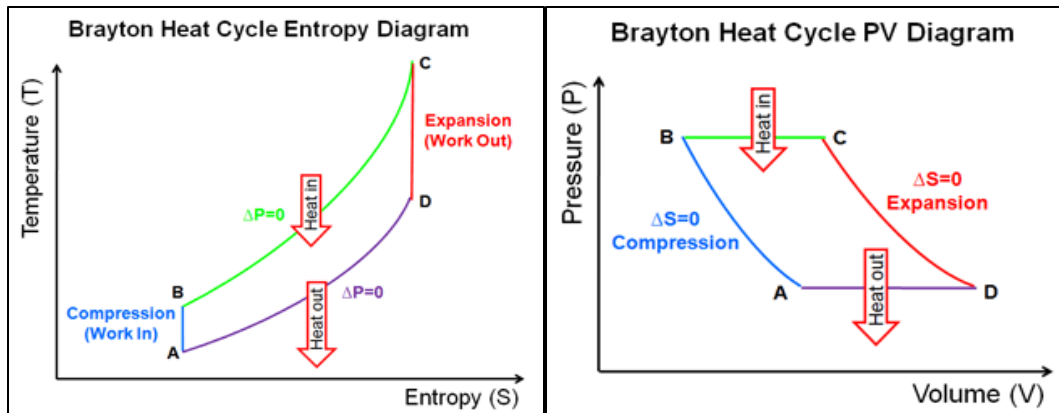


Figure 2.7: (a) and (b) Brayton Cycle

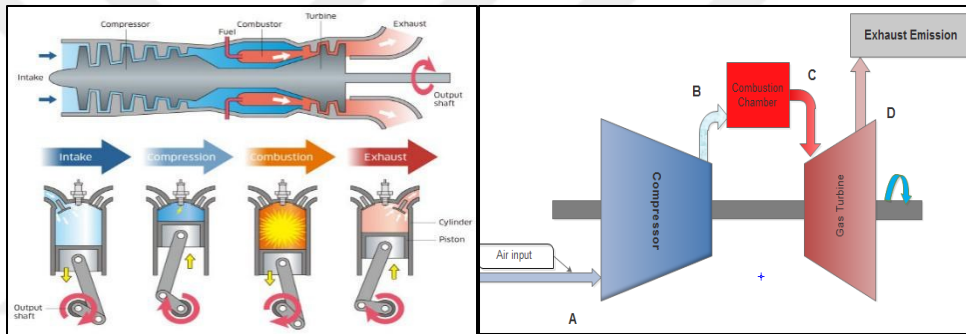


Figure 2.8: (a) and (b) Application Brayton Cycle

2.6.1. Gas turbine cycles

The ideal cycle that the working fluid undergoes in this closed loop is the Brayton cycle, which is made up of four internally reversible processes:

(A-B) Is the isentropic compressing, the air is compressed through the axial compressor (Air drawn into the turbine and compressed in the compressor stage).

(B-C) Is the Constant-pressure combustion or heat addition (Fuel mixed with the high pressure air in the combustion chamber and burned at constant pressure).

(C-D) Is the Isentropic expansion (in the turbine) (Hot gases expand in the turbine stages.)

(D-A) Is the Constant-pressure heat rejection. (Constant pressure ejection of the spent, hot gases to the environment.)

This cycle (Brayton cycle) may be characterized by two quantities: the peak

temperature in the cycle T_c and the ratio of pressures $r = \frac{P_B}{P_A} = \frac{P_C}{P_D}$

If we assume that the working fluid in this cycle is an ideal gas then from basic thermodynamic theory we know that:

$$PV = mRT \quad (2-1)$$

$$PV^\gamma = \text{Constant (this is true on an adiabatic process)} \quad (2-2)$$

Using equations (1) and (2), it can be shown quite readily that:

$$\frac{T_B}{T_A} = \frac{T_C}{T_D} = \left(\frac{P_B}{P_A}\right)^{\frac{\gamma-1}{\gamma}} = \left(\frac{P_C}{P_D}\right)^{\frac{\gamma-1}{\gamma}} \quad (2-3)$$

Where γ is the ratio of specific heats of the gas (for air this constant = 1.4). Ideally, γ is a constant. In a real gas turbine cycle it varies throughout the cycle as a function of the working fluids chemical composition and temperature. However, for simplicity it is assumed here that it is a constant value.

The temperature T_C is the highest temperature in the cycle and may be assumed to be the notional temperature of the hot gases entering the first stage of the turbine. In practice, this temperature will need to be kept below a certain limit in order to preserve the life of (reduce fatigue and stress on) the hot gas-path parts in the turbine. However, it is extremely difficult to measure this temperature in practice since insertion of thermocouples with a fast response time into this region of the turbine can be difficult, and there is not one temperature but rather a spread of temperatures across the combustion chamber/cans. Therefore, it is common to measure the temperature at the exhaust of the turbine (T_D), and through controlling of this temperature T_C is maintained below its limit. Based on equation (3), if there is a set limit on T_C then the limit on T_D will vary as a function of pressure ratio r . That is,

$$T_D \text{ limit} = T_C \text{ limit} \left(\frac{1}{r}\right)^{\frac{\gamma-1}{\gamma}} \quad (2-4)$$

In practice the processes involved are more complex and variations in γ , evaluation of fluid friction etc. can not be ignored and thus the relationship between the cycle temperatures is also more complex. However, the basic concepts are the same and thus typically modern gas turbine controls will limit the exhaust temperature of the turbine as a function of the cycle pressure ratio [54],[55].

Therefore, in general the exhaust temperature limit of the gas turbine will be implemented as a monotonic function of pressure ratio, i.e.:

$$T_D \text{ limit} = f(r) \quad (2-5)$$

The exhaust temperature is governed by airflow into the combustion chamber and the fuel burnt.

The airflow through the turbine can be adjusted by changing the angular position of the inlet guide vanes (IGVs). In a combined-cycle power plant the IGVs are modulated during part load conditions. This reduces the airflow and thus keeps exhaust temperature high at reduced loading levels to maintain the desired level of the heat transfer into the heat recovery steam generator; this helps to maintain an overall higher plant efficiency [40]. Once the gas turbine is loaded close to base load, the IGVs become wide open. At this point the control of the turbine fuel flow is taken over by a temperature control loop which acts to control the fuel in order to maintain the exhaust temperature at its limit. In a simple-cycle turbine the IGVs are wide-open throughout most of the units loading cycle. Thus, for comparable turbines at the same part-load condition, the exhaust temperature of a combined-cycle unit is higher than that of a simple-cycle unit. The consequence of this is that if a frequency excursion were to occur the resultant transient overshoot in turbine power would be higher on the simple-cycle unit since it would have started at a temperature significantly lower than its combined-cycle counterpart. However, the final steady-state power output of both turbines would be the same once they reach, and settle down, at their temperature limit.

2.6.2. Characteristics of Axial Compressor Flow

Consider equation (88). From this equation it can be seen that the term RT has the physical units of meter squared per seconds-squared ($m^2 \cdot s^{-2}$). Now if we take the speed of the compressor blades in revolutions per second (Hz) and multiply this by the length of the compressor rotor blade (L) and then divide this number by the square root of RT , we have:

$$\eta = \frac{\omega L}{\sqrt{RT}} \quad (2-6)$$

Which is a dimensionless quantity. Furthermore, since the speed of sound in a fluid $=\sqrt{\gamma RT}$, then η can be physically interpreted as the speed of the tip of the compressor rotor blades to the ratio of the speed of sound (i.e. a Mach number [40]). Similarly, a dimensionless quantity can be established for the rate of mass flow of air into the compressor

$$\phi = \frac{\dot{m}\sqrt{RT}}{AP} \quad (2-7)$$

Where A is exposed area at the inlet of the compressor, P is the air pressure at the inlet and \dot{m} is the mass flow of air (in $\text{kg}\cdot\text{s}^{-1}$). Furthermore, since

$$\dot{m} = \rho Av \quad (2-8)$$

Where ρ is the density of air and v the velocity of air, and from equation (2-7) $P = \rho RT$, then equation (2-9) can also be written as

$$\phi = \frac{v}{\sqrt{RT}} \quad (2-9)$$

Which physical represents the relative speed of the air entering the compressor to the speed of sound (again a Mach number).

These quantities together with pressure and temperature ratios characterize the compressor. The advantage of this characterization is that the temperature and speed dependency of the compressor airflow can be represented as one monotonic function. This is graphically shown in Figure 2.9. The dimensionless airflow versus speed characteristic of an example turbine can be found in [49]. The significance of this representation is that for example the operating condition defined by η_1 and ϕ_1 (see Figure 2.9) can be reached by either decreasing shaft speed in order to arrive at $\eta = \eta_1$ or by raising ambient temperature relative to the reference condition under which η is defined = 1.0 pu. Note, however, that although the dimensionless airflow for two such conditions is similar the actual airflow for a higher temperature condition will be less due to the lower air density.

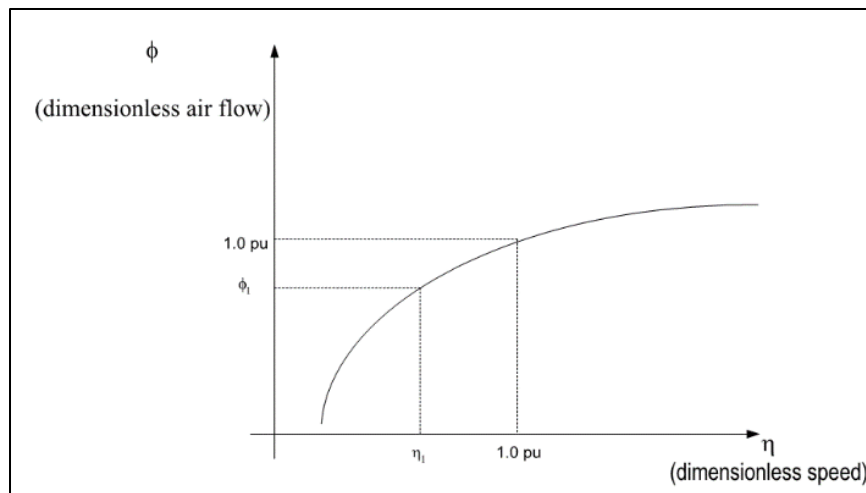


Figure 2.9: Compressor Airflow Characteristics

This information, i.e. the airflow versus speed curve for a compressor, is not readily available but there is a potential for identifying this relationship through field test [49].

2.6.3. Deviation of Actual Gas-Turbine Cycles from Idealized Ones

The genuine gas-turbine cycle contrasts from the perfect Brayton cycle on a few records. First off, some weight drop amid the warmth expansion and warmth dismissal procedures is inescapable. All the more vitally, the genuine work contribution to the compressor is more, and the real work yield from the turbine is less in light of irreversibility.

The deviation of genuine compressor and turbine conduct from the glorified isentropic conduct can be precisely represented by using the isentropic efficiencies of the turbine and compressor as.

$$\eta_C = \frac{w_s}{w_a} \cong \frac{h_{2s} - h_1}{h_{2a} - h_1} \quad (2-10)$$

$$\eta_T = \frac{w_a}{w_s} \cong \frac{h_3 - h_{4a}}{h_3 - h_{4s}} \quad (2-11)$$

Where states $2a$ and $4a$ are the actual exit states of the compressor and the turbine, respectively, and $2s$ and $4s$ are the corresponding states for the isentropic case, as illustrated in Figure 2.10.

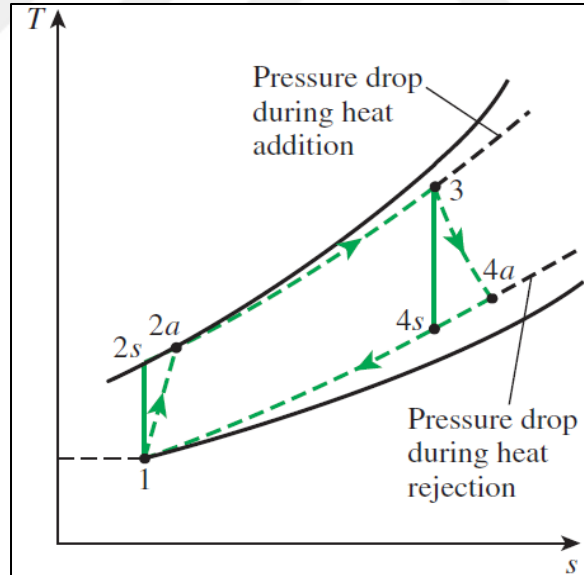


Figure 2.10: The Deviation of An Actual Gas-Turbine Cycle From The Ideal Brayton Cycle As A Result of Irreversibilities.

2.6.4. Modification in The Simple Cycle

We have discussed simple cycle in the previous pages and found that the heat of exhaust gases is a waste, if it is not used by modifying the cycle, Also for higher power

generation or say for multistage compression and expansion if intercooling and reheating are not used, the output can not be increased. Therefore in practical gas turbine power plant accessories such as exchanger, intercooler and heaters are used to increase efficiency and output.

2.6.5. Gas Turbine Modeling

The dynamic turbine modelling has focused on the turbine component in a gas turbine power plant simulator. Thus, the turbine model was built up by smaller model components to predict the turbine dynamic behavior at different operating conditions. Turbine blade cooling was studied using an air stream injecting from compressor outlet to the turbine stator and rotor to avoid high thermal stress on the stage. However, this was made on the expense of a power output loss. This is fully consistent with the conclusions of [56] that for low and medium gas turbine power plants, blade cooling can be omitted.

2.7. Overview on Turbine Frame 9

The gas turbine is the most versatile item of turbomachinery today. It can be used in several different modes in critical industries such as power generation, oil and gas, process plants, aviation, as well domestic and smaller related industries. A gas turbine essentially brings together air that it compresses in its compressor module, and fuel, that are then ignited. Resulting gases are expanded through a turbine. That turbine's shaft continues to rotate and drive the compressor which is on the same shaft, and operation continues. A separate starter unit is used to provide the first rotor motion, until the turbine's rotation is up to design speed and can keep the entire unit running.

The compressor module, combustor module and turbine module connected by one or more shafts are collectively called the gas generator. In land-based industries, gas turbines can be used in either direct drive or mechanical drive application. With power generation, the gas turbine shaft is coupled to the generator shaft, either directly or via a gearbox "direct drive" application. A gearbox is necessary in applications where the manufacturer offers the package for both 60 and 50 cycle (Hertz, Hz) applications. The gearbox will use roughly 2 percent of the power developed by the turbine in these cases.

In power generation applications, a gas turbine's power/ size is measured by the power it develops in a generator (units watts, kilowatts, Megawatts). In mechanical drive applications, the gas turbine's power is measured in horsepower (HP), which is essentially the torque developed multiplied by the turbine's rotational speed.

The combination of compressor module, combustor module and turbine module is termed the gas generator. Beyond the turbine end of the gas generator is a freely rotating turbine. It may be one or more stages. It is not mechanically connected to the gas generator, but instead is mechanically coupled, sometimes via a gearbox, to the equipment it is driving. Compressors and pumps are among the potential "driven" turbomachinery items. See Figure 2.11 below.

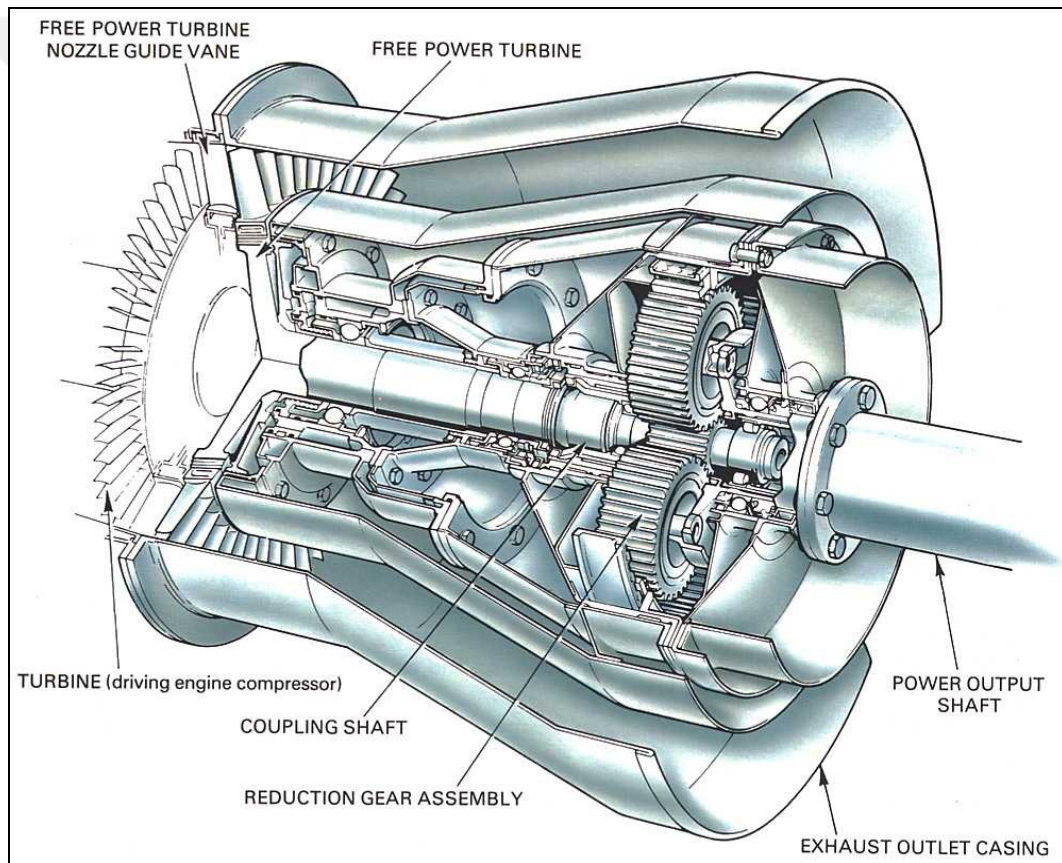


Figure 2.11: A typical Free Power Turbine. (Source: Rolls-Royce, UK)

The technical specification of the turbine of this study can be listed as in the following table (Table 2.1).

Table 2.1: Technical Specification of The Turbine

General Operation Conditions	
Atmospheric Pressure	1012
Design ambient temperature	50° centigrade
Minimum ambient temperature	-6° centigrade
Maximum ambient temperature	55° centigrade
Design relative humidity	30%
Minimum relative humidity	5%
Maximum relative humidity	95%
Seismic code	UBC97
Grid code	No specific requirement

Gas Turbine	
Frame size	PG9171
Fuel system	Dual fuel (natural gas +light diesel oil)
Starter	Electrical motor
Air filtration	Self-cleaning
Compressor /turbine cleaning	On and off –line compressor water wash and off-line turbine washing
Exhaust system	Side right
Fire protection	High pressure CO_2
Generator	
Model	Model GE9A5, Brush BDAX9, or Alston T900B as a function of availability
Frequency	50Hz
Power factor	0.85 lagging
Power factor	Up to 0.95 leading
Terminal voltage	15 KV
Control Systems	
Gas turbine	Speedtronic Mark VIe(TMR)

Estimated Performance – Base Load , Liquid Fuel				
Estimated Performance- PG9171				
Load Condition		Base	Base	Base
Exhaust static pressure	mm H ₂ O	106.7	75.6	72.4
Ambient temperature	deg C	-0.5	50	55

The complexity of power plant operation, of their interaction with the electrical network, as well as the need of implementing coordinated control systems to cope with specific operational requirements, call for the development/use of advanced and accurate simulation tools. This may represent the adequate complement or substitute the practice of repetitive prototyping and expensive tests on real systems. Within this context, the parameter identification of power plant dynamic models represents one of the main issues for proper simulation of the transients occurring during critical operation conditions. This work deals with a parameter-identification procedure conceived for the development of a computer-based simulator aimed at reproducing the islanding and black-startup energization transients of a power system consisting of a combined cycle power plant, the local distribution network and relevant loads.

In particular, the computer simulator refers to a 80 MW power plant composed by two aero-derivative gas turbine (GT) units and a steam turbine unit (ST) in combined cycle. The simulator represents the dynamic behavior of the GTs, the heat recovery steam generator, the ST and their control systems. Concerning the electrical apparatus, it includes the model of the synchronous generators along with their exciters, automatic voltage regulators (AVRs), as well as the representation of the local electrical network (step up unit transformers, cable link between the power plant substation and distribution substation and loads) connected to the external transmission network.

As the first step of modelling and control, it is necessary to get enough information about the type of the modelled gas turbine. Although there are different types of GTs based on their applications in industry, they have some main common parts including combustion chamber, compressor and turbine. The set of these components is called engine core or gas generator (GG). Compressor and turbine are connected with the central shaft and rotate together.

GTs are divided into two main categories including aero gas turbines (jet engines) and stationary gas turbines. In aero industry, the gas turbine is used as the propulsion system to make thrust and to move an airplane through the air. Thrust is usually generated based on the Newton's third law of action and reaction. There are varieties of aerogas turbines including turbojet, turbofan, and turboprop. If the main shaft of the GG is connected to an electro generator, it can be used to produce electrical power. Industrial power plant gas turbines are playing a key role in producing power, especially for the plants which are far away on oil fields and offshore sites where there is no possibility for connecting to the general electricity network. GGs may also be tied to large pumps or compressors to make turbo-pumps or turbo compressors respectively.



CHAPTER THREE

GAS TURBINE IDENTIFICATION BY ANN

3.1. Overview

Artificial neural network models for gas turbines can be formed using different methods based on the flexibility that artificial neural networks provide. This flexibility is depends on the number of neurons, the number of hidden layers, values of the biases and weights, type of the activation function, the structure of the network, algorithms and training styles as well as data structure. On the other hand, the best structure is the one which can predict behaviour of the system as accurately as possible.

Choosing the right parameters of gas turbines (GTs) as outputs and inputs of the NN is very significant for making a reliable and accurate model. The availability of data for the selected parameters, Knowledge of the system to determine the interconnection between different objectives and parameters for model making are the key factors in selecting appropriate outputs and inputs. Accuracy of the Choosing output parameters can be examined by sensitivity analysis.

There are different approaches and methodologies in system identification and modelling of industrial systems. Artificial neural network (ANN) is increasingly considered as a suitable alternative to white-box models over the last few decades. The nature and strength of the interrelations of system variables as well as the nature of applications are vital criteria for training a neural network with sufficiently rich empirical data. The general methodology that follow can be described in Figure 3.1.

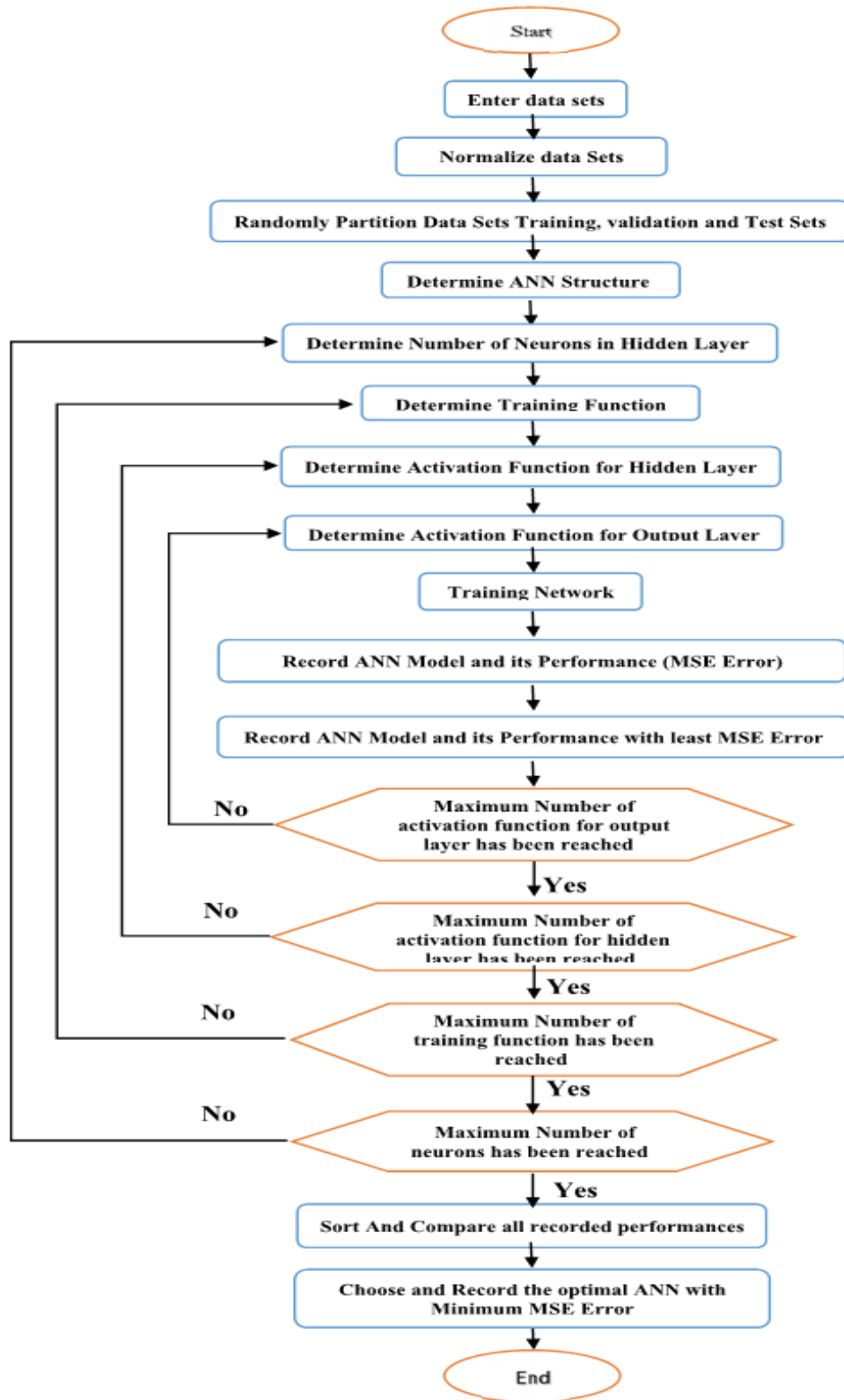


Figure 3.1: Flow Diagram of The Adopted ANN Methodology in System Identification

3.2. Custom Neural Network

Artificial neural networks are computational analogues of small biological neural systems that possess useful computational properties. In particular, it is possible to train a neural network on example data such that the neural network can subsequently map inputs correctly to outputs that were not present in its training set. In this way it is possible to build a model of a complicated physical system, such as a gas turbine engine, without drawing from any prior knowledge of the physics of the system. Although we know a great deal about the physics of the gas turbine, the explicit calculation of degradation influences from the available performance data is ambiguous and so this ability to model an engine purely from the data it provides is useful.

In this research, the neural network used is a custom feed-forward network with the input propagating through the network to produce an output. Later it will be described how errors are back-propagated from the output of the model to the input and it is important to note that the terms ‘input’ and ‘output’ are fixed in relation to the network geometry. A feedforward neural network with sigmoidal activation functions approximates any mapping with a differentiable neural network function. It is the differentiability of the neural network model that makes it suitable for optimization of the engine. The calculation of the values of the derivatives can be done by a simple extension to the existing error back- propagation algorithm used for training neural networks.

3.3. Methodology

The complexity of real neurons is highly abstracted when modelling artificial neurons. These basically consist of inputs, which are multiplied by weights, and then computed by a mathematical function which determines the activation of the neuron.

The backpropagation algorithm is used in layered feedforward ANNs. This means that the artificial neurons are organized in layers, and send their signals “forward”, and then the errors are propagated backwards. The network receives inputs by neurons in the input layer, and the output of the network is given by the neurons on an output layer. There may be one or more intermediate hidden layer. The backpropagation algorithm uses supervised learning, which means that we provide the

algorithm with examples of the inputs and outputs we want the network to compute, and then the error (difference between actual and expected results) is calculated. The idea of the backpropagation algorithm is to reduce this error, until the ANN learns the training data. The training begins with random weights, and the goal is to adjust them so that the error will be minimal.

The first step to formulate the problem is the identification of proper inputs and output sets. According to relations between the turbine parameters' observations such as; air temperature, Fuel Consumption, and Inlet Guide Vane position as input signals and electrical output power of gas turbine as output signals.

3.3.1. ANN Design

In this work, a Custom Neural Network used for the simulation and training the process. A custom Feed forward network is chosen for implementing the artificial neural network (ANN). Three inputs at the input layer, hidden layer and output layer respectively. Some hidden layers are taken and number of neurons vary from 4 to 20 in each layer in order to arrive at final architecture. After sufficient experimentation and simulation, one hidden layer is selected. The hidden layer contains four neurons in related to three inputs, Fuel, inlet guide fan, and exhaust temperature, while the output layer contains one neuron in related to one output which represented by the Plant output power (Mwatt). The neural network architecture is displayed in Figure 3.2.

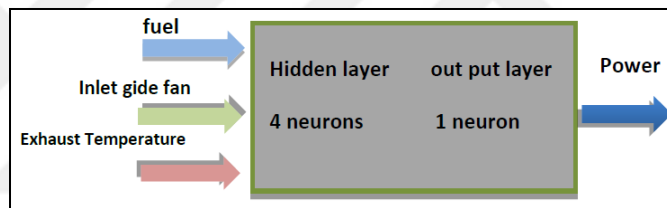
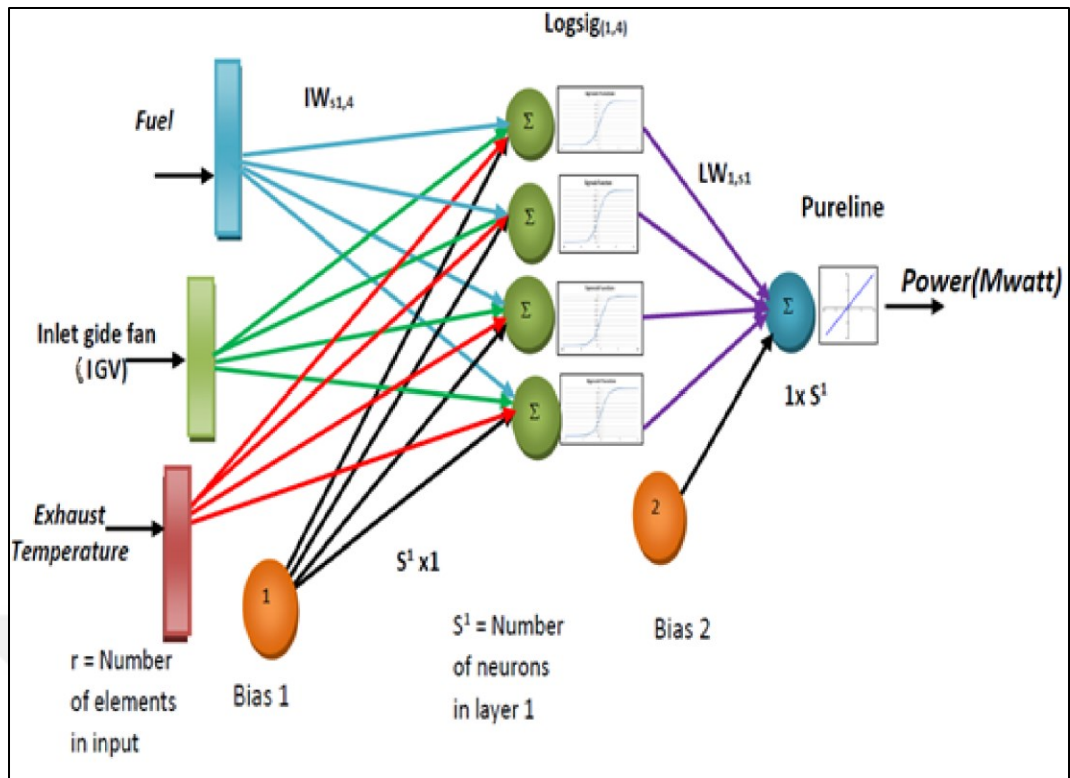


Figure 3.2: One-Layer Network With Three Inputs, Four Neurons, and One Output neuron (Power)

3.3.2. Training algorithm

For better performance of the proposed neural network design, all inputs and output data have been normalized, then, they are used in the neural network training procedure. Eighty percent of data are used for training, ten percent of input is used for validating and ten percent of data are used for testing network. All Input and output data are gathered from logging system and operational documents from real Power Plant. The training algorithm can be expressed in a form of a block diagram as shown in Figure 3.3.

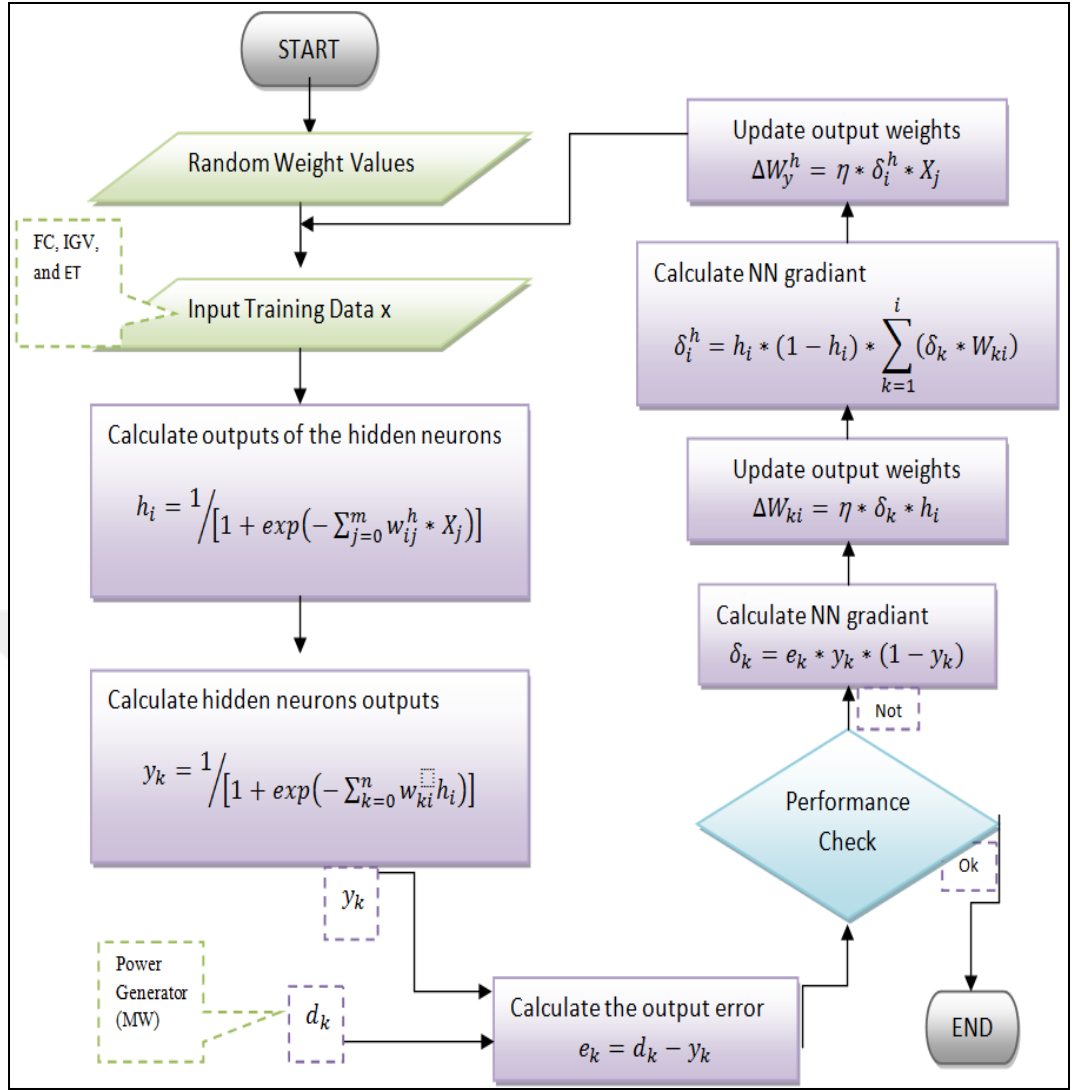


Figure 3.3: Training Algorithm of The Proposed Custom Neural Network.

3.3.3. Deriving Model Equation

This part of the work wants to present a general data-driven method for formulating suitable model equations for gas turbine as a nonlinear complex system. The method is validated in a quantitative way by its application to experimentally measured data. We have developed the gas turbine power formula as a function of the variables on which it mainly depends, that are: Fuel (F), Exhaust Temperature (ET) and Inlet Guide Vane (IGV). A log-sigmoid activation function is used for the neurons of the hidden layer, while the linear function for the output layer neurons to simplify the solutions. Therefore, for the hidden layer:

$$f_1(n) = \text{logsig}(n)$$

$$f_2(n) = \text{pureline}(n)$$

Where $f_1(n)$ and $f_2(n)$ denote to the activation function of n-th neuron in the hidden and output layers respectively. The input layer is a three-dimensional vector represented by: the Fuel (F), Exhaust Temperature (ET), and the Inlet Guide Vane (IGV). Thus, for the configuration of Figure 3.3, whereas 3 input parameters, 4 hidden neurons, and one output neuron, the neurons' output equations at the hidden layer ($A_1^1 \dots A_4^1$), are as follows:

$$n_1^1 = F * Iw_{(1,1)} + ET * Iw_{(1,2)} + IGV * Iw_{(1,3)} + b_{(1,1)}^1 \quad (3-1a)$$

$$A_1 = 1 / (1 + e^{(-n_1^1)}) \quad (3-2a)$$

$$n_2^1 = F * Iw_{(2,1)} + ET * Iw_{(2,2)} + IGV * Iw_{(2,3)} + b_{(2,1)}^1 \quad (3-1b)$$

$$A_2 = 1 / (1 + e^{(-n_2^1)}) \quad (3-2b)$$

$$n_3^1 = F * Iw_{(3,1)} + ET * Iw_{(3,2)} + IGV * Iw_{(3,3)} + b_{(3,1)}^1 \quad (3-1c)$$

$$A_3 = 1 / (1 + e^{(-n_3^1)}) \quad (3-2c)$$

$$n_4^1 = F * Iw_{(4,1)} + ET * Iw_{(4,2)} + IGV * Iw_{(4,3)} + b_{(4,1)}^1 \quad (3-1d)$$

$$A_4 = 1 / (1 + e^{(-n_4^1)}) \quad (3-2d)$$

Where all $n_1^1 \dots n_4^1$, $A_1^1 \dots A_4^1$, represent the neurons input summation function and the activation functions of the hidden layer respectively. At the output layer:-

$$\begin{aligned} \mathbf{Power}_{output} &= A_1 * Lw_{(1,1)} + A_2 * Lw_{(1,2)} + A_3 * Lw_{(1,3)} \\ &\quad + A_4 * Lw_{(1,3)} + A_{1,1}^2 * b_{(1,1)}^2 \end{aligned} \quad (3-3)$$

$$A_1^2 = f_2(n_1^2) = \text{pureline}(n_1^2) = 1 \quad (3-4)$$

Where the n_1^2 , A_1^1 , represent the neurons input summation function and the activation functions of the output layer respectively.

Where \mathbf{Power}_{output} , denotes to the model output power which resulting from training the weights; I_w , L_w , b^1 , b^2 , that are associated with the input, hidden and the bias respectively.

Mean Squared Error (MSE): is the criteria that used to stop the training process, on which the loop terminates when minimum desired error occurs. The standard reference MSE is used to calculate the performance of the networks. It represents the average squared difference between initial target values and achieving output values from open loop mode.

$$MSE = \frac{1}{t} \sum_{i=1}^t (\check{y}_{r(i)} - y_{r(i)})^2 \quad (3-5)$$

Where the $\check{y}_{r(i)}, y_{r(i)}$, denote the observations and the modeling outcome data respectively.

Correlation Coefficient (R): it measures the correlation between the correct outputs and those provided by the network; as R is closer to 1 as the approximation is better. The value of the correlation coefficient can be expressed as in (3.6).

$$R = \frac{n \sum \check{y}y - (\sum \check{y})(\sum y)}{\sqrt{n(\sum \check{y}^2) - (\sum \check{y})^2} \sqrt{n(\sum y^2) - (\sum y)^2}} \quad (3.6)$$

Where n is the number of pairs of data.

3.4. Results and Network Performance

A two cases have been addressed for modelling in this part, the first, when training the proposed custom ANN on 3 main inputs (Fuel (F), Exhaust Temperature (ET) and Inlet Guide Vane (IGV)), while the second, trained at five input parameters (Fuel Consumption (FC), Fuel Percentage (FP), Exhaust Temperature (ET), Inlet Guide Vane (IGV), and Compressor Air Pressure (Cp)).

3.4.1. Case 1, (3 inputs)

After conducting the simulation for more than seven times while comparing the custom ANN outcome with the measurements, Best performance index with a minimum error occurred at 45 Epochs (number of training iterations) with performance value equals to 0.643, which indicates the value on which the iteration process has stopped (the value of MSE) this process with the network weights training can be seen in Figure 3.4.

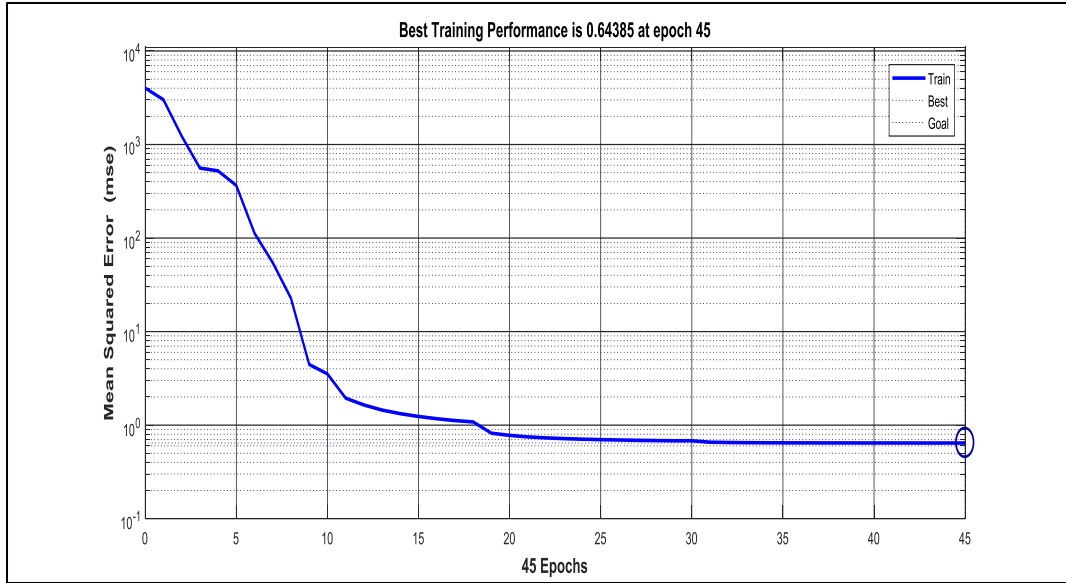


Figure 3.4: Training Process Along With Performance Index Measuring For 3 Inputs.

To get the mathematical modelling equation for the system model, the weights' vectors of the layers for the custom ANN has been extracted as follow:

$$I_w = \begin{bmatrix} 13.3 & -5.6179 & -3.3508 \\ -0.69582 & -2.0788 & 0.31162 \\ 0.00045481 & 0.094982 & 0.00023654 \\ -2.5308 & 7.4064 & 0.11496 \end{bmatrix}$$

$$b_1 = [-18.331, 4.5183, 1.7403, -8.0575]$$

$$L_w = [-1.5129; -912.35; 2028; 34.579]$$

$$b_2 = -885.01$$

Where I_w , b_1 , L_w , b_2 represent the input layer, input bias, hidden layers, and output bias weights respectively. The simulation results of the output power can be calculated from solving the resultant algebraic equations. Therefore, after some substitutions and simplifications, the mathematical modelling equations of the power can be given by:

Power

$$\begin{aligned} &= \frac{2027.9528}{0.17546 * e^{(-0.09498249682 * LGV)} + 1} \\ &- \frac{912.35}{0.0109 * e^{(2.0788 * LGV)} * e^{(0.69582 * F)} * e^{-0.31162 * Et}} \\ &- \frac{1.51289}{9145262.55 * e^{(5.61787 * LGV)} * e^{(3.3508 * Et)} * e^{(-13.29982 * F)} + 1} \\ &+ \frac{34.5786}{3157.538 * e^{(2.5307 * F)} * e^{(-7.406387 * LGV)} * e^{(-7.406387 * LGV)} * e^{(-0.11496 * Et)} + 1} \\ &- 885.0101 \end{aligned}$$

The comparison between the simulated and the predicted data which also called the correlation coefficient can be seen in Figure 3.5

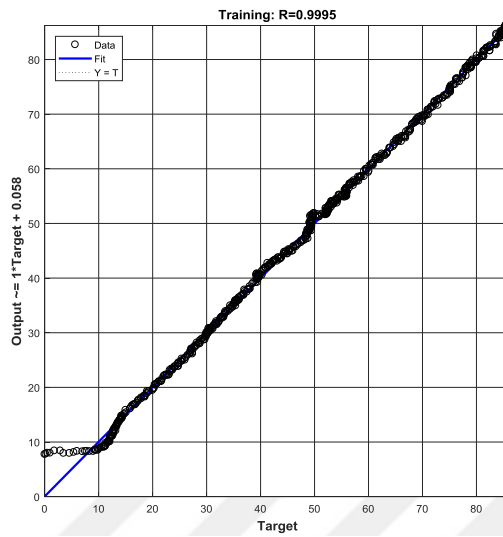


Figure 3.5: Comparison Between Simulated and The Predicted.

3.4.2. Case 2, (5 inputs)

Several simulation processes have been conducted while also comparing the custom ANN outcome with the measurements to get best performance index with a minimum error. It is found that; after 175 Epochs (number of training iterations), performance index value approach to 0.141, the process during the network training for the weights can be seen in Figure 3.6.

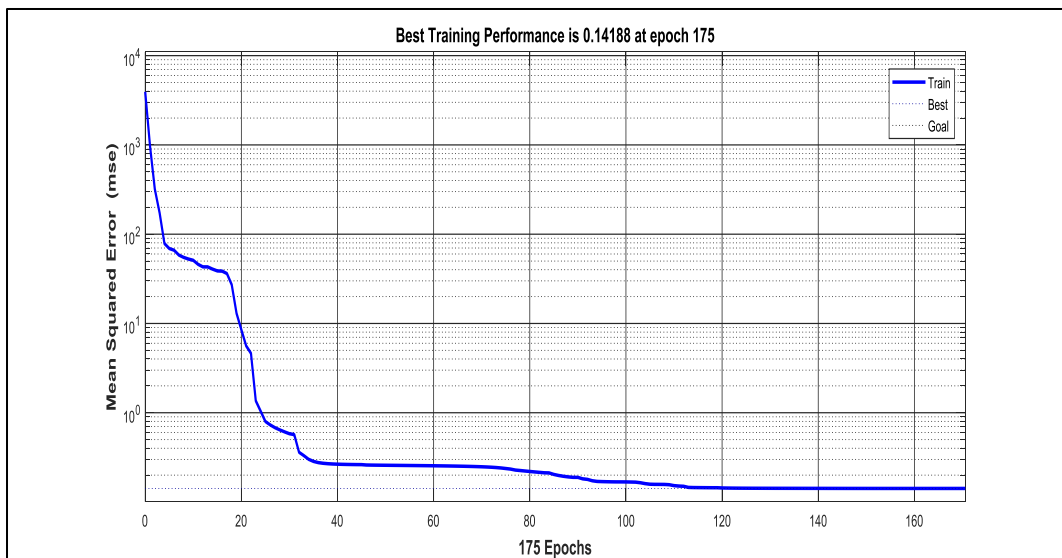


Figure 3.6: Training Process Along With Performance Index Measuring For 5 Inputs.

To get the mathematical modelling equation for the system model, the weights' vectors of the layers for the custom ANN has been extracted as follow:

$$I_w = \begin{bmatrix} 0.8075 & -0.4150 & 2.0339 & 0.8931 & 1.1604 \\ 0.7315 & 0.4089 & -3.3787 & -0.1995 & 0.1577 \\ -0.0043 & 0.0063 & -0.0036 & -0.0104 & -0.3216 \\ 0.1705 & 0.9799 & -7.0593 & -1.6297 & 1.1510 \end{bmatrix}$$

$$b_1 = \begin{bmatrix} -16.5654 \\ -27.1018 \\ 4.1898 \\ 4.2818 \end{bmatrix}$$

$$L_w = [66.7025 \quad -0.3444 \quad -172.4861 \quad 6.4324]$$

$$b_2 = [73.2855]$$

Thus, the power equation due to the network outcome be:

$$\begin{aligned} \mathbf{Power} = & 66.702 / (\exp(0.414 * IGV - 0.893 * FP - 1.160 * Cp - \\ & 0.807 * FC - 2.033 * ET + 16.565) + 1.0) - 0.344 / (\exp(0.199 * FP - \\ & 0.408 * IGV - 0.157 * Cp - 0.731 * FC + 3.378 * ET + 27.101) + 1.0) + \\ & 6.432 / (\exp(1.629 * FP - 0.979 * IGV - 1.151 * Cp - 0.170 * FC + 7.059 * \\ & ET - 4.281) + 1.0) - 172.486 / (\exp(0.010 * FP - 0.006 * IGV + 0.321 * \\ & Cp + 0.004 * FC + 0.003 * ET - 4.189) + 1.0) + 73.285 \end{aligned}$$

The comparison between the simulated and the predicted data output can be seen in Figure 3.7.

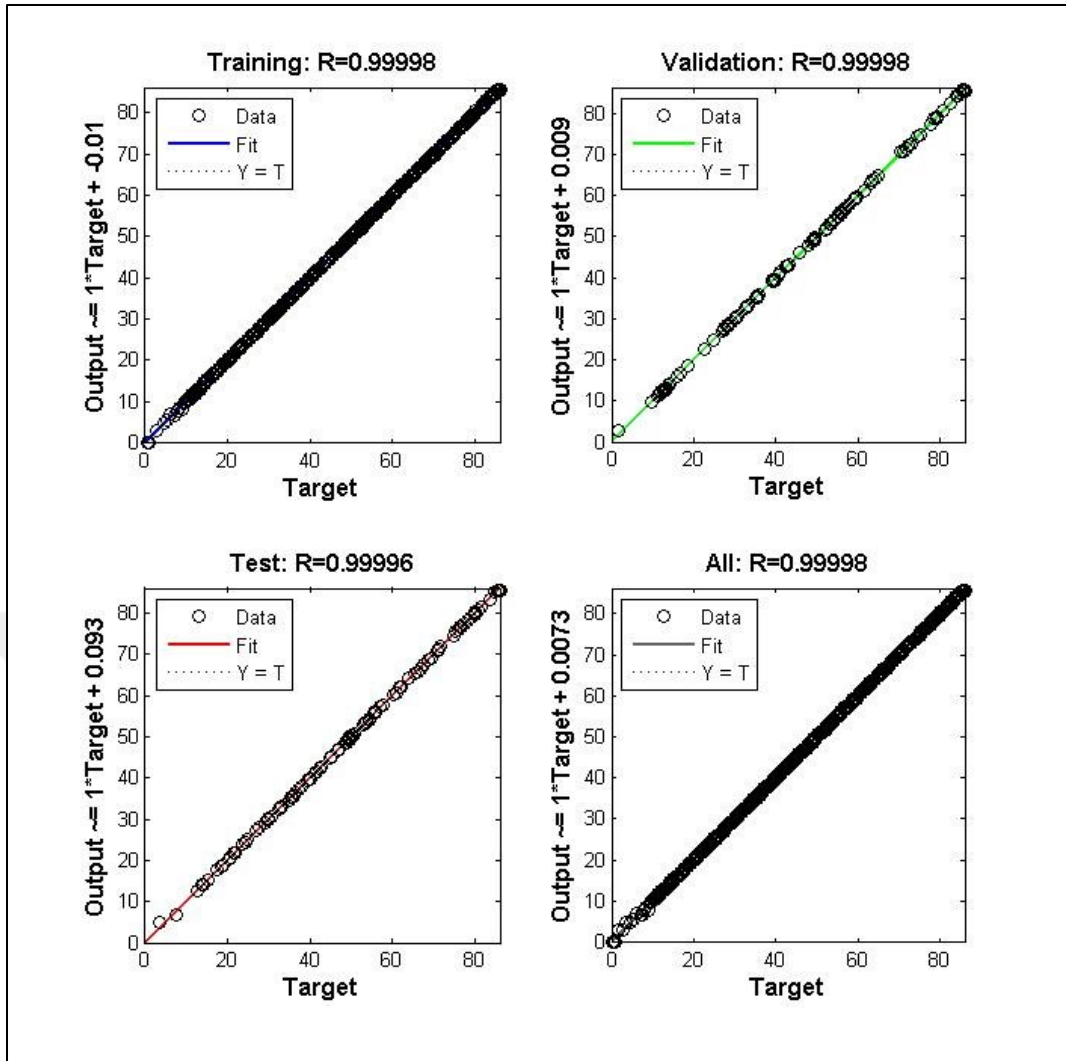


Figure 3.7: Comparison Between Simulated and The Predicted.

While the field measurements compared with the model outcome data can be shown in Figure 3.8.

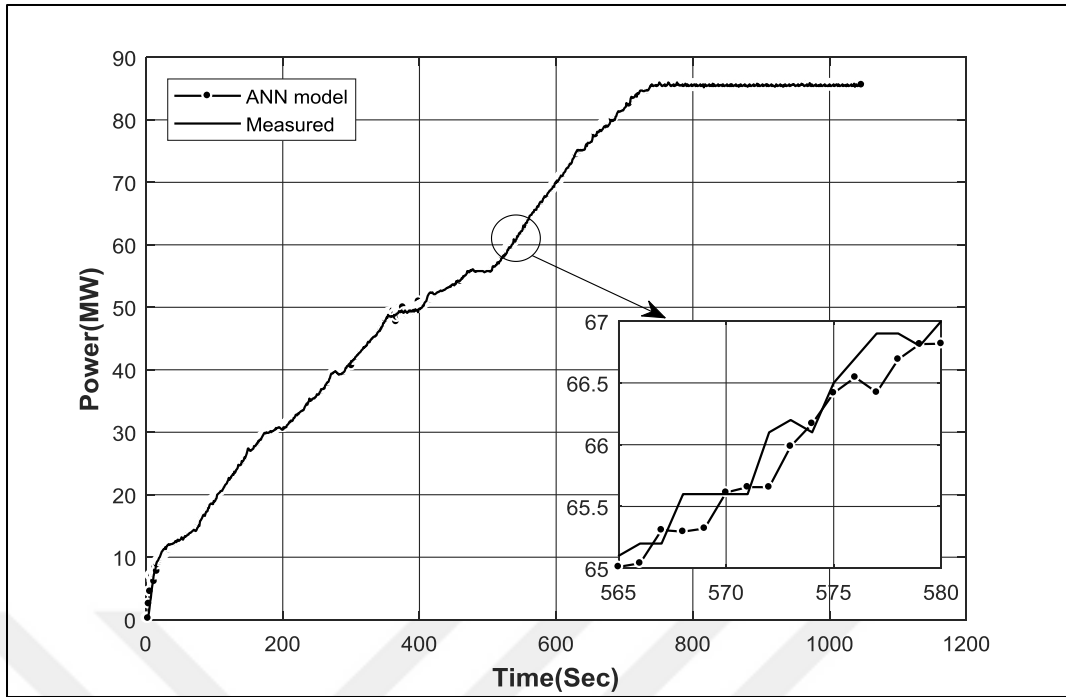


Figure 3.8: Comparison of Data Fields Measurements and Network Power (Mwatt) With Time (Sec).

Another interpretation of the approximation range of the custom ANN model structure is the error curve over the sampling time with can be shown in Figure 3.9.

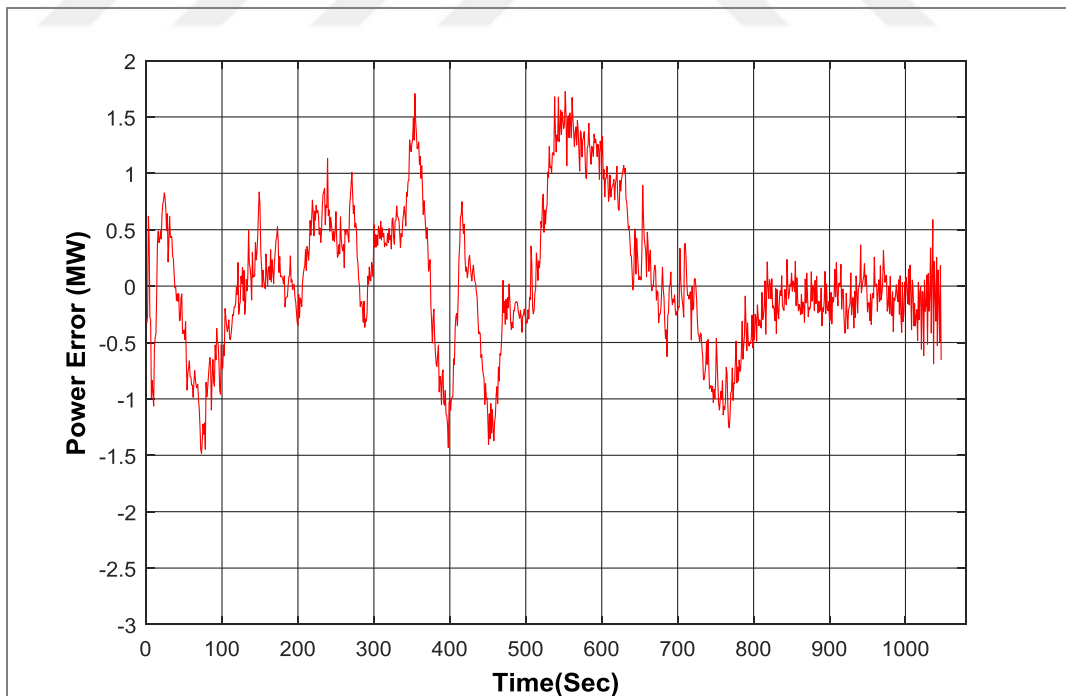
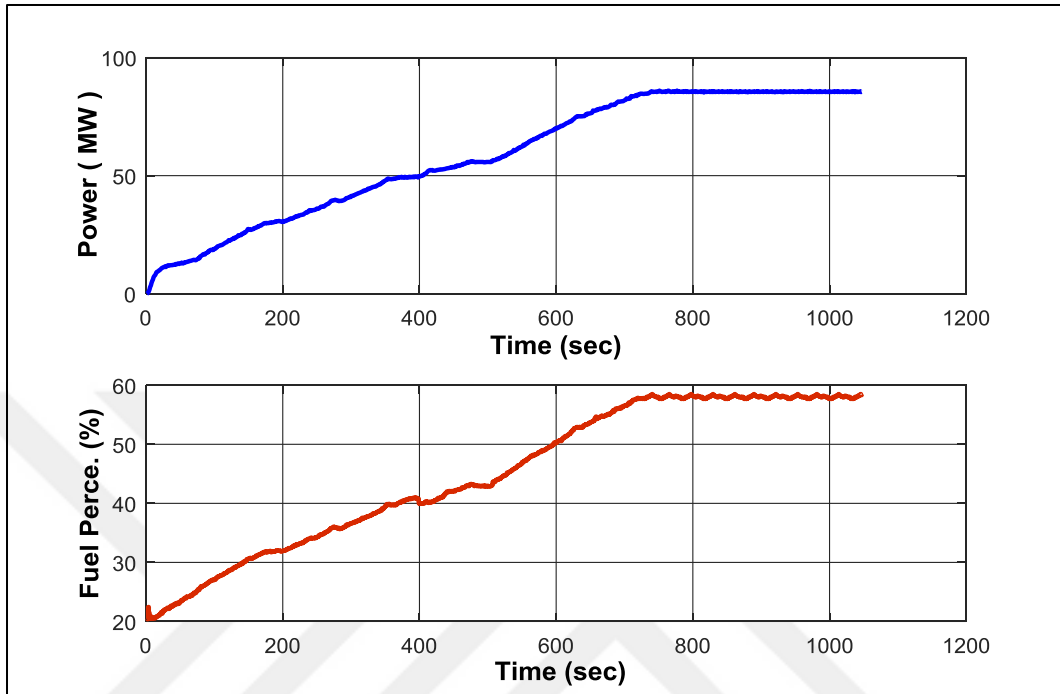


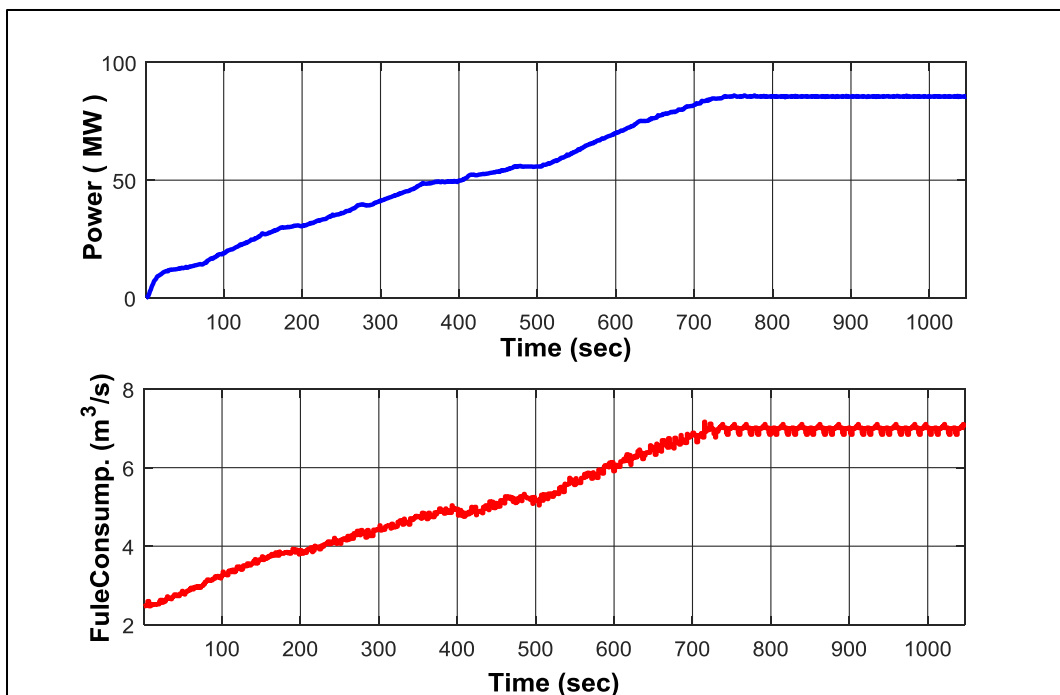
Figure 3.9: Error Curve of Custom ANN Model

Furthermore, and to clarify the response of the output model formula with respect to each input individually, the following figures demonstrate these relations

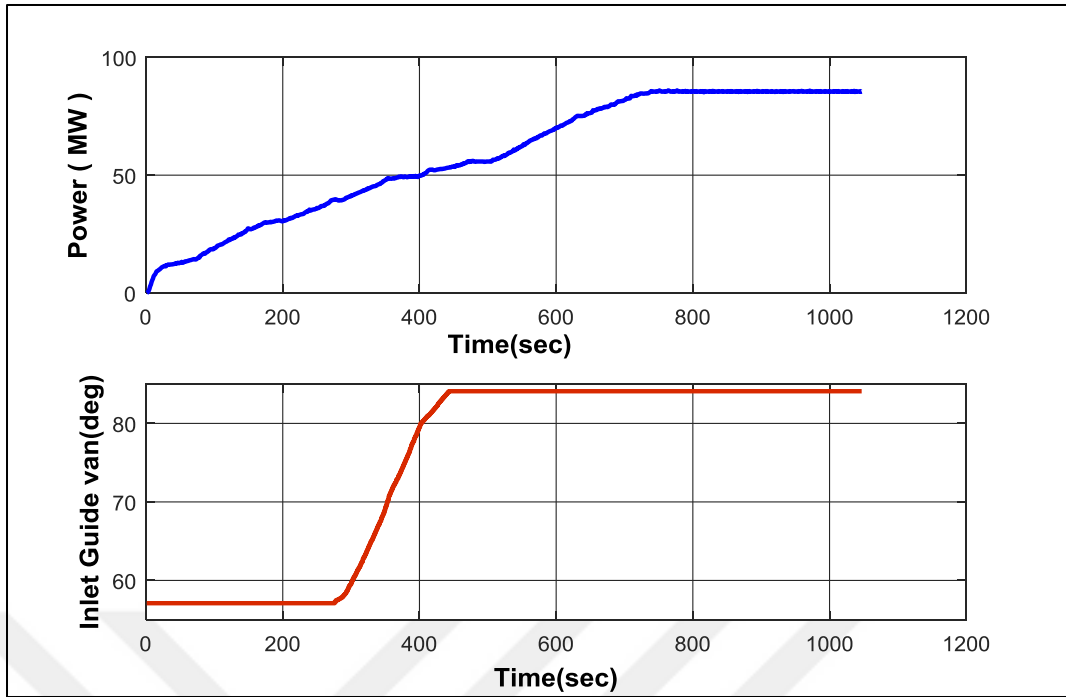
between the power output from one side, and with respect to Fuel Consumption (FC), Fuel Percentage (FP), Exhaust Temperature (ET), Inlet Guide Vane (IGV), and Compressor Air Pressure (Cp). As can be seen in Figure 3.10 (a,b,c,d, and d)



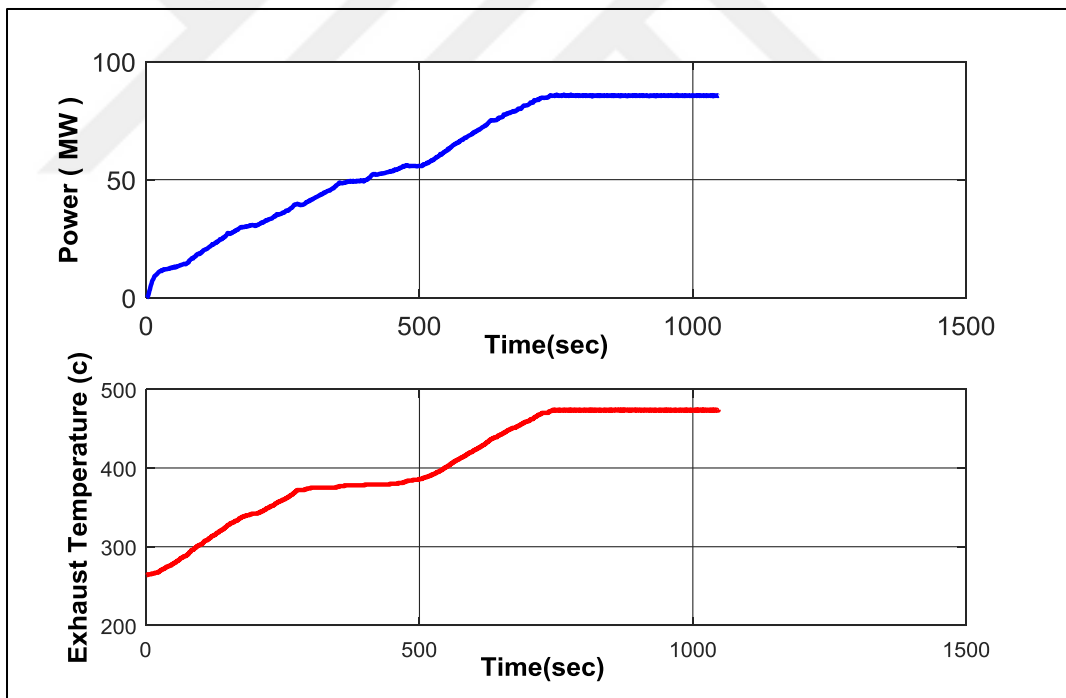
(a)



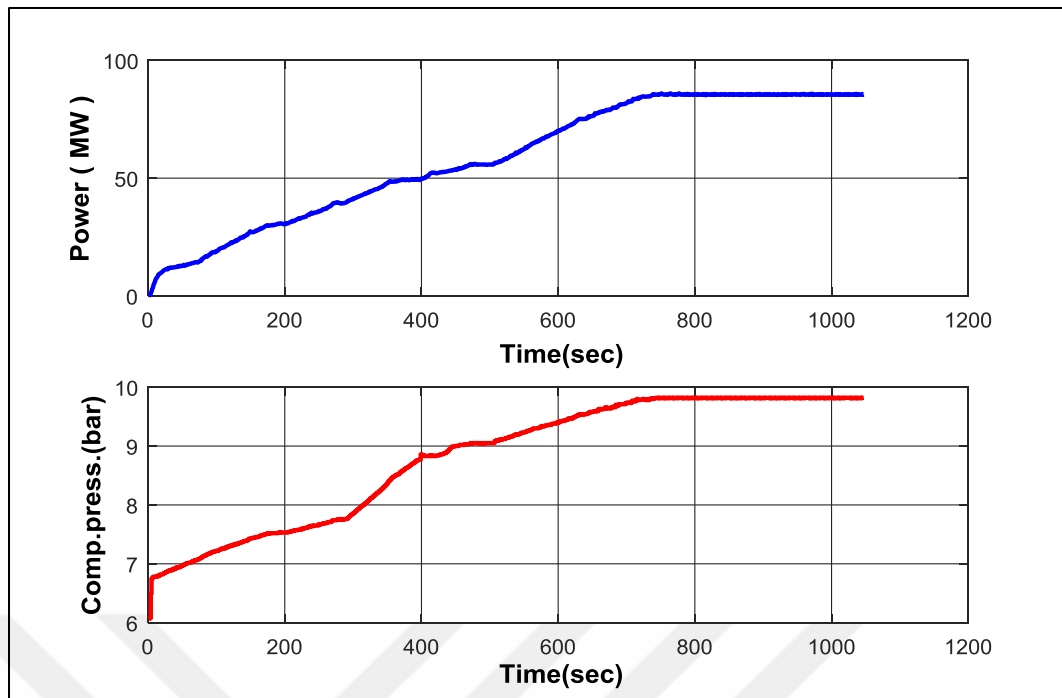
(b)



(c)



(d)



(e)

Figure 3.10:The Model Output Power With Respect to Each Input: (a) Fuel Consumption (FC), (b) Fuel Perce (FP), (c) Exhaust Temperature (ET), (d) Inlet Guide Vane (IGV),and (e) Compressor Air Pressure (Cp)

3.5. Summary

A custom ANN technique is applied to the GT system, which described in the previous section, to extract a model shows the effect of the system input parameters on the output power. The target of using Custom ANN is achieved when the power modeling equation has been obtained. The function complexity depends on the number of inputs and their interactive relationships among them, and also the number of selected hidden neurons in the network. The linear activation function of the output neuron simplifies the solution of the algebraic equations that equivalent to the number of hidden neurons that in turn add the nonlinearity behavior of the network to model that due to system measurements.

Data sampling is made from full speed no load to full load (86.17 MW base load) conditions with sampling interval 1.0 sec. Gas turbine behaviors are extremely depends on fuel consumption and ambient condition, and the experiments showed that the ambient temperature is a crucial parameter. Based on simulation results, it is found that the ANN model can describe the system behaviors adequately.

The resulting model showed that the existing artificial neural network method can be reliably process to determine the system of gas turbine systems. The gas turbine

output parameters can reasonably be predicted based on changes in system inputs. The approach of this study can also be used to predict performance of similar gas turbine systems with high accuracy when training from real data obtained from this type GT frame 9. This is particularly useful when real data is only available over a limited operational filed.



CHAPTER FOUR

LINEAR AND NONLINEAR IDENTIFICATION MODELS OF GAS TURBINE

4.1. Introduction

The primary focus of this dissertation is the development of methods to extract simple linear dynamic models of system dynamics suitable for condition monitoring and control design of industrial gas turbines. This is an inherently nonlinear application and we cannot trivialize or ignore the nonlinear characteristic of the machinery. To accommodate the nonlinear characteristics, the interconnection of the fuel system and turbine engine is approximated by a block Hammerstein system for the identification of fuel valve contamination.

Linear dynamic models have been demonstrated to capture the dominant dynamics of gas turbine behavior and to be suitable for the design of diagnostic algorithms. For example, high-fidelity models can be used for modelling the fuel control subsystem, or alternatively viewed as a black-box system shown in a simple block diagram as shown in Figure 4.1. This, or similar, simplified block structure approximations will be used throughout the discussion due to the relative simplicity and utility. Example closed loop black-box system, where P is the plant, K the controller, with reference r , control output $u(t)$, input noise d , plant input u , plant output y , measurement noise v , and measurement z .

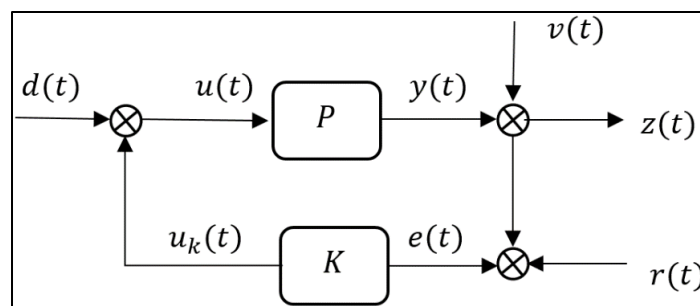


Figure 4.1: Sample Control System Block Diagram

A mathematical model is called continuous-time when it describes the relationship between continuous time signals. Continuous-time models are shown with a function $f(t)$ that changes over continuous time. A model is called discrete-time when it directly expresses the relationships between the values of the signals at discrete instants of time. The relationship between signal values is usually expressed by using differential equations. In practical applications, signals are most often obtained in sampled form in discrete time measurements.

4.1.1. Linear System Identification

The object's static and dynamic characteristics, static and dynamic nonlinearities and characteristics' sensitivity to operating parameters must be accounted while identifying the dynamic object. The model structure is composed by using theoretical studies, and the parameters from test data are estimated. Usually, power system dynamic model structures are known and can be described by linear or nonlinear differential equations. The task of identification is to determine numerical values of the model parameters. The response of linear system output can be described by the sum of responses to separate input signals. According to the input signal type, the object's response can be described as transient function $h(t)$, impulse function $g(t)$, transfer function – frequency response function $W(j\omega)$, autocorrelation function $R_{xy}(\tau)$ and spectral density function $S_{xy}(\omega)$. All these characteristics are interdependent, but the object dynamic parameters are estimated in a different way because of noises, inaccurate and insufficient test data. The parametric identification methods are used for identification of dynamic models in the transient investigation of the power system. Non-parametric identification methods, e.g. correlation or spectral density analysis may be used for estimation of generalized parameters.

Identification of the frequency domain method is based on Fourier transformation. The task of identification in time domain is the determination of the transient function between input and output signals. If the object's input and output signals are stationary processes and are measured discretely, the object model can be written as

$$y(t) = G(q, \theta)u(t) + H(q, \theta) e(t) \quad (4-1)$$

where q : shift operator; θ : transfer function parametric vector, $e(t)$: sequence of random unrelated data [57],[58].

Parametric identification methods. The generalized parametric model is described by expression:

$$A(q)y(t) = \frac{B(q)}{F(q)}u(t) + \frac{C(q)}{D(q)}e(t), \quad (4-2)$$

Where $y(t)$: output signal, $u(t)$: input signal, $e(t)$: signal error or noise, q : shift operator and $A(q)$, $B(q)$, $C(q)$, $D(q)$ and $F(q)$ – polynomials [2].

Partial cases of the model (4-2) can be used, assuming that some of the polynomials $A(q)$, $B(q)$, $C(q)$, $D(q)$ and $F(q)$ are equal to 1 (Table 4.1). If the discrete parametric identification method is used, the polynomials of the identified model, (4-2), are transformed into continuous time model polynomials.

Relationship between parameter vectors of discrete and continuous time functions depend on z and s operators.

The parameters θ_g and θ_h of discrete generalized parametric model partial cases response function $G(q, \theta_g)$ and $H(q, \theta_h)$ are identified using sampled input and output signals $u(t)$ and $y(t)$. The main transient function $G(q, \theta_g)$ of identified discrete model is converted into continuous time domain transfer function $\widehat{W}(s, \hat{\theta})$. The parametric vector $\hat{\theta}$ of the continuous time model is determined from the expression

$$\hat{\theta} = \arg \min_{\theta} \sum_{i=0}^{n-1} (y(t+1) - \hat{y}(t+1), \theta)^2. \quad (4-3)$$

Table 4.1: Most Frequent Cases of Partial Parametric Model

Model structure	Polynomials
FIR(finite impulse response)	B(q)
ARX	A(q),B(q)
ARMAX	A(q),B(q),C(q)
ARMA	A(q),C(q)
ARARX	A(q), B(q), D(q)
ARARMAX	A(q), B(q), C(q),D(q)
OE(output error)	B(q), F(q)
BJ (Box-Jenkins)	B(q), F(q), C(q), D(q)

The identified model must meet three similarity conditions:

- The autocorrelation of output signals of measured and simulated identified transfer function must converge towards 1, and the least square criterion must be as small as possible:

$$\begin{aligned}
 R &= \text{corr}(y(t), \hat{y}(t)) \rightarrow 1 \\
 S &= \sum_{i=0}^{n-1} (y(t+i) - \hat{y}(t+i))^2 \rightarrow 0
 \end{aligned}
 \quad \left. \vphantom{\begin{aligned} R \\ S \end{aligned}} \right\} \quad (4-4)$$

Where

$y(t)$: measured output signal; $\hat{y}(t)$: simulated output signal of the identified transfer function $\widehat{W}(s, \hat{\theta})$ when the input of the transfer function is measured signal $u(t)$; S : least square coefficient, R : autocorrelation coefficient.

4.1.2. Nonlinear System Identification

A Hammerstein model is a specialized model structure where a nonlinear system is approximated by a series connection of a static memory less nonlinear function in series with a linear dynamic plant. The Hammerstein model structure is relevant to many engineering applications where nonlinear behavior is the rule rather than the exception. Most physical devices have nonlinear characteristics outside a limited linear range. Control elements, such as valves and position actuators, are typically linear in a limited operating range and possess some form of saturation, hysteresis, or nonlinear characteristics in the input/output characteristic.

In addition, it is common to approximate a dynamic nonlinear system with a linear dynamic model around a local operating point. The linear models may be obtained via linearization of a known nonlinear model or by experimentation and identification methods.

The performance of the fuel control system in a gas turbine engine is critical to maintain stability and achieve performance targets. A digital feedback controller meters fuel into the combustion chamber using measurements of shaft speed, stage temperatures, pressures, and power. The fuel control valve(s) typically possess a nonlinear position to flow area relationship. The control system requires knowledge of this nonlinear characteristic to accurately regulate fuel flow. Uncertainty or degradation of the physical fuel valve's flow characteristic can lead to instability or operational limitations of the turbine engine. Maximization of machine availability is

essential for operators and the cost of unplanned service interruption is typically greater than the cost of preventative maintenance and returning the unit to service. The motivation of this research is the identification of turbine parameters in a nonlinear actuator characteristic in closed-loop operation. Hammerstein model framework. The Hammerstein model structure comprises an input nonlinearity in series with a linear dynamic model. This model structure can be used to identify the turbine parameters nonlinearity and approximate the dynamics of the turbine engine via a linear plant model. Identification of closed-loop Hammerstein systems has focused on instrumental variable based methods as they mitigate the bias due to the correlation of output noise and the input and output signals.

4.2. Transfer Function Identification

This model shows how to deal with field experimental data with several input and output channels (MIMO data). The common operations, such as viewing the MIMO data, estimating and comparing models, and viewing the corresponding model responses are highlighted. This data set is collected from a Field scale Turbine engine. It has several inputs such as; Comp.Air Pressure (Cp) in (bar), ExhTemp (ET) in (°C), FulePerce (FP) in (%), Inlet Gide Vane (IGV) in (deg), Fuel Consumption (FC) in (m^3/sec). As a biginning, we'll consider the most effective parameters that represented by ET, FC, defined as above. The output is the generated power and the sampling time was 1 (sec).

4.2.1. The fitting percentage

The fitting percentage can be expressed as the fitting value of estimation experimental data and calculated using:

$$\text{fit} = 100\left(1 - \frac{\|y - \hat{y}\|}{\|y - \text{mean}(y)\|}\right) \quad (4-5)$$

Where y is the validation data output and \hat{y} is the output of the system.

4.2.2. Akaike's Final Prediction Error (FPE)

Akaike's Final Prediction Error (FPE) criterion provides a measure of model quality by simulating the situation where the model is tested on a different data set.

After computing several different models, you can compare them using this criterion. According to Akaike's theory, the most accurate model has the smallest FPE.

If you use the same data set for both model estimation and validation, the fit always improves as you increase the model order and, therefore, the flexibility of the model structure.

Akaike's Final Prediction Error (FPE) is defined by the following equation:

$$FPE = \det \left(\frac{1}{N} \sum_{t=1}^N e(t, \hat{\theta}_N) (e(t,))^T \right) \left(\frac{1+d/N}{1-d/N} \right) \quad (4-6)$$

Where:

- N is the number of values in the estimation data set.
- $e(t)$ is a ny -by-1 vector of prediction errors.
- $\hat{\theta}_N$ represents the estimated parameters.
- d is the number of estimated parameters.

The method that has been adopted in the estimation process is nonlinear least squares with automatically chosen line search. To gain some preliminary insight into the data characteristics, we started by evaluating a default-order discrete model which assumes 2 poles and 1 zero for each transfer function. The input/output delay has been extracted from the real measurements of the field data (Generator Power). Therefore, to estimate the parameters of the addressed turbine system, we need to identify the following:

Data has 1 output given by (Generator Power). 2 inputs given by (Exhaust Temperature and Fuel Consumption). Number of samples are 1047. Thus, Transfer functions with poles given by: [2 2], and zeros: [1 1], while the I/O delay: [1 1].

First, we've collected the measured channels into an iodate object:

At a sample time: 1 seconds, the Discrete-time identified transfer functions are as follows:

From input "Exhaust Temperature" to output "Gen. Power":

$$G1 = q^{-1} * \frac{-0.0001243 q^{-1}}{1 - 1.914 q^{-1} + 0.9152 q^{-2}}$$

While from input "Fuel Consumption" to output "Gen. Power":

$$G2 = q^{-1} * \frac{0.782 q^{-1}}{1 - 0.1159 q^{-1} - 0.8479 q^{-2}}$$

The fitting to estimate experimental data was: 94.45%, FPE: 2.017, and Mean Square Error (MSE): 1.992.

4.2.3. Pole Zero Map

For basic information about the inspection of system stability, we can use the pole-zero map as can be seen Figure 4.2.

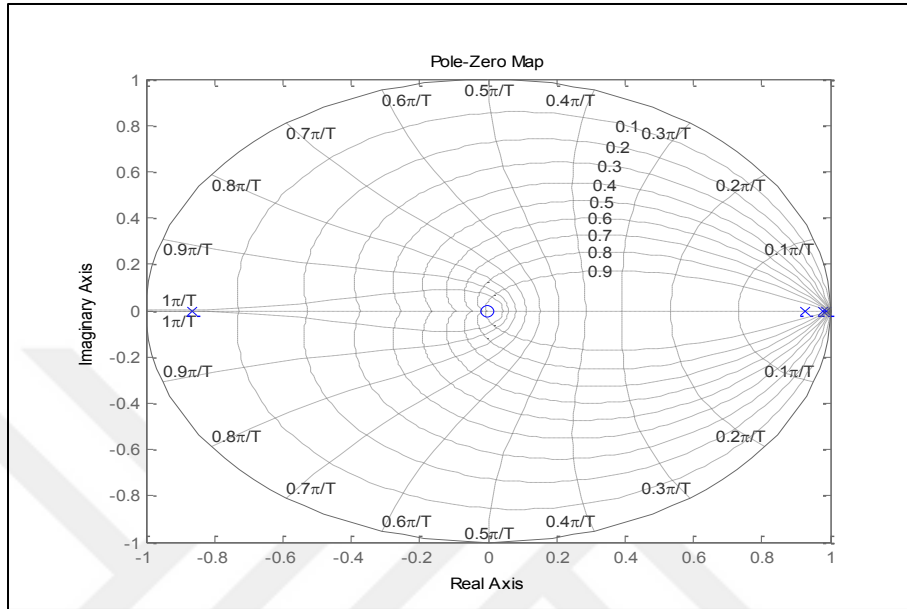


Figure 4.2: Pole-Zero Map

To plot the simulated response of a dynamic system model to the field experimental data, a time response comparison between the validation/Output power (Gen. Power) and the Model estimated (tf3) can be seen in Figure 4.3.

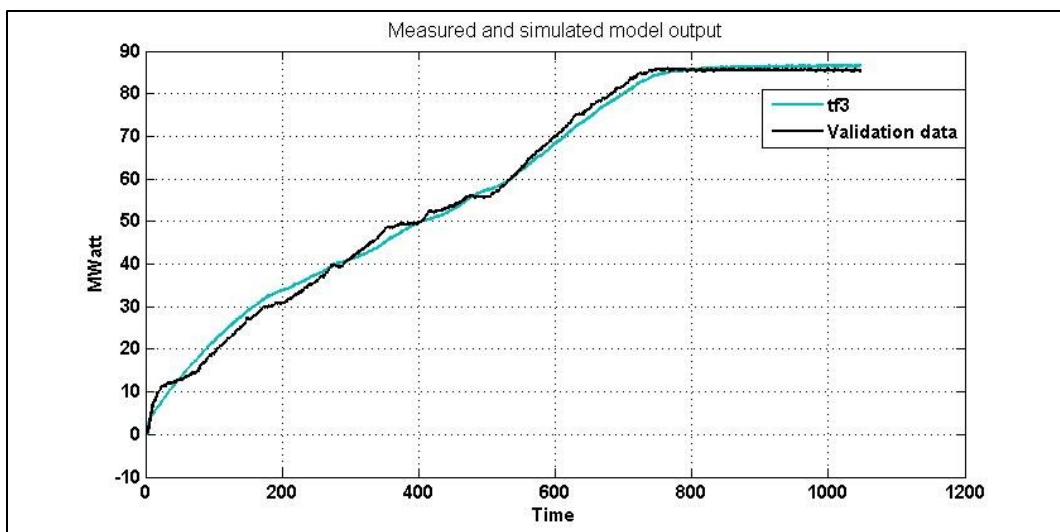


Figure 4.3: Time Response Comparison Between The Validation/Output Power (Gen. Power) and The Model Estimated (tf3)

4.2.4. Step and Impulse Responses

The step and the impulse responses of the estimated transfer function model can be seen in Figure 4.4.

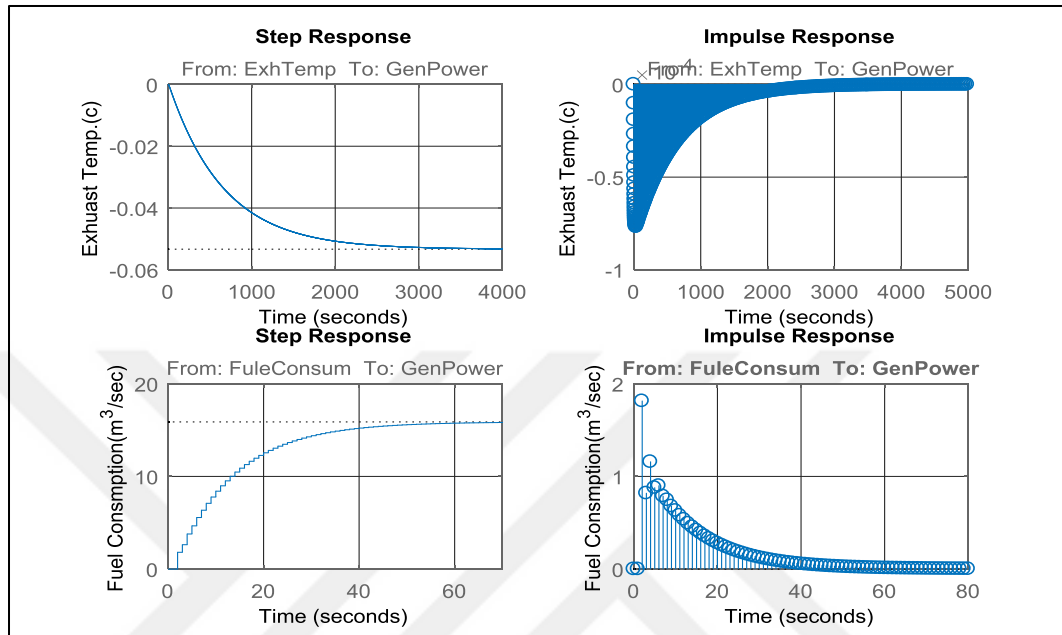


Figure 4.4: Step and Impulse Responses

Where the rise and settling time have been indicated on the step response of the plot as well as the confidence region.

4.3. Determining whether the system is stable

The system has been tested according to the above time and frequency analysis and the distribution of its poles and zeros of the estimated model, and in a short and confident decision, we used the function $STB = \text{is stable}(tf3)$ to check the stability and it is a stable system ($STB=1$)

4.4. State Space

State-space models are very useful for dynamic systems; that is, systems with responses that are time functions. Wiberg (1971) and Zadeh and Desoer (1963) give general discussions of state-space models. Tim can be treated as either a continuous or

where a_{ij} are the coefficients and b_{ij} are constants that describe the system. This set of n equations defines the derivatives of the state variables to be a weighted sum of the state variables and the system inputs. Equations (4-6) may be written compactly in a matrix form:

$$\frac{d}{dt} \begin{bmatrix} x_1 \\ x_2 \\ x_3 \\ \vdots \\ x_n \end{bmatrix} = \begin{bmatrix} a_{11} & a_{12} & \cdots & a_{1n} \\ a_{21} & a_{22} & \cdots & a_{2n} \\ a_{31} & a_{32} & \cdots & a_{3n} \\ \vdots & \vdots & \ddots & \vdots \\ a_{n1} & a_{n2} & \cdots & a_{nn} \end{bmatrix} \begin{bmatrix} x_1 \\ x_2 \\ x_3 \\ \vdots \\ x_n \end{bmatrix} + \begin{bmatrix} b_{11} & \cdots & b_{1r} \\ b_{21} & \cdots & b_{2r} \\ b_{31} & \cdots & b_{3r} \\ \vdots & \ddots & \vdots \\ b_{n1} & \cdots & b_{nr} \end{bmatrix} \begin{bmatrix} u_1 \\ \vdots \\ u_r \end{bmatrix} \quad (4-9)$$

The general form is :

$$\dot{x}(t) = Ax(t) + Bu(t) \quad (4-10)$$

$$y(t) = Cx(t) + Du(t) \quad (4-11)$$

The matrix A is called the stability matrix. B is called the control matrix, and C and D are called state and control observation matrices, respectively.

4.5. Estimate state-space models

The applied data set is collected from a field scale Turbine engine. It has several inputs such as; Compressor Air Pressure (Cp) in (bar), Exhaust Temperature (ET) in (°C), Fule Percentage (FP) in (%), Inlet Gide Vane (IGV) in (deg), Fuel Consumption (FC) in (m^3/sec).

The state-space model is in the innovations form as in the following:

$$x(t + Ts) = A x(t) + B u(t) + K e(t) \quad (4-12)$$

$$y(t) = C x(t) + D u(t) + e(t) \quad (4-13)$$

If we assume that: $m = (\text{data}, \text{order})$

m : The resulting model as object.

Data: An iodate object containing the output-input data.

Order: The desired order of the state-space model. If order is entered as a row vector (like $\text{order} = [1:10]$), preliminary calculations for all the indicated orders are carried out. A plot will then be given that shows the relative importance of the dimension of the state vector. More precisely, the singular values of the Hankel matrices of the impulse response for different orders are graphed. The idea is to choose an order such that the singular values for higher orders are comparatively small.

4.6. Results of State Space Estimation

We evaluate the system identification of the state space model through two selections of system order, 6th and 2nd.

4.6.1. 6th order state space model:

The model can be extracted by using the following function:

$$Dt = m(\text{Turbine}, 6^{\text{th}})$$

Where Dt is the Discrete-time identified state-space model which is given by:

$$x(t + Ts) = A x(t) + B u(t) + K e(t)$$

$$y(t) = C x(t) + D u(t) + e(t)$$

The state space matrices are:

$$A = \begin{bmatrix} -0.9943 & -0.122 & -0.1147 & -0.01322 & 0.0412 & -0.06808 \\ 0.008958 & -0.8416 & -0.4598 & 0.02681 & 0.2348 & -0.2817 \\ -0.0213 & -0.06195 & -0.3118 & -0.5727 & 0.1352 & 0.5323 \\ -0.01224 & -0.03751 & -0.124 & -0.3988 & -0.6464 & -0.09283 \\ -0.005661 & -0.06676 & -0.514 & -0.6569 & -0.4587 & -0.2404 \\ 0.01114 & 0.0903 & 0.1115 & -0.1185 & 0.4911 & -0.7373 \end{bmatrix}$$

	ExhTemp	FulePerce	FuleConsum	Comp.press.	Inlet Gid.vane
$B =$	0.002344	0.01175	0.002625	0.09157	-0.007331
	0.005084	0.02942	0.01137	0.1777	-0.01042
	-0.005143	-0.03055	-0.01069	-0.0184	-0.01994
	0.001228	0.001982	0.03497	0.1077	-0.09494
	-0.0002276	-0.004193	-0.02865	-0.006642	-0.1083
	0.001897	0.02288	0.01563	0.08402	-0.1654

$$C = [15 \quad 1.243 \quad -1.433 \quad 0.5997 \quad -0.7291 \quad -0.5136]$$

$$D = [0 \quad 0 \quad 0 \quad 0 \quad 0 \quad 0]$$

From input "Exhaust Temperature" to output "Power":

$$\frac{0.04878 s^5 + 0.1396s^4 - 0.1422s^3 - 0.06761s^2 - 0.01987s + 0.004107}{s^6 + 3.742 s^5 + 5.284 s^4 + 3.594 s^3 + 1.425 s^2 + 0.5013 s + 0.1285}$$

From input "Fuel Percentage" to output "Power":

$$\frac{0.2491s^5 + 0.6865s^4 - 0.6577s^3 - 0.2899s^2 - 0.08888s + 0.02185}{s^6 + 3.742 s^5 + 5.284 s^4 + 3.594 s^3 + 1.425 s^2 + 0.5013 s + 0.1285}$$

From input "Fuel Consumption" to output "Power":

$$\frac{0.1027s^5 - 0.3265s^4 - 0.5194s^3 - 0.5771s^2 - 0.3706s + 0.09142}{s^6 + 3.742s^5 + 5.284s^4 + 3.594s^3 + 1.425s^2 + 0.5013s + 0.1285}$$

From input "Compressed Pressure" to output "Power":

$$\frac{1.647s^5 + 4.295s^4 - 3.977s^3 - 2.182s^2 - 1.172s + 0.3509}{s^6 + 3.742s^5 + 5.284s^4 + 3.594s^3 + 1.425s^2 + 0.5013s + 0.1285}$$

From input "Inlet Guide Vane" to output "Power":

$$\frac{0.01263s^5 - 0.3529s^4 + 0.9548s^3 + 0.728s^2 + 0.02701s - 0.08191}{s^6 + 3.742s^5 + 5.284s^4 + 3.594s^3 + 1.425s^2 + 0.5013s + 0.1285}$$

The Sample time of the measurements is 1 seconds, The Comparison between the state space model and the measurements can be seen in Figure 4.6, and the evaluation parameters to measure how close the model from the measured data can be described by:

Fit to estimation data: 99.33% (prediction focus)

FPE: 0.03325, MSE: 0.02909

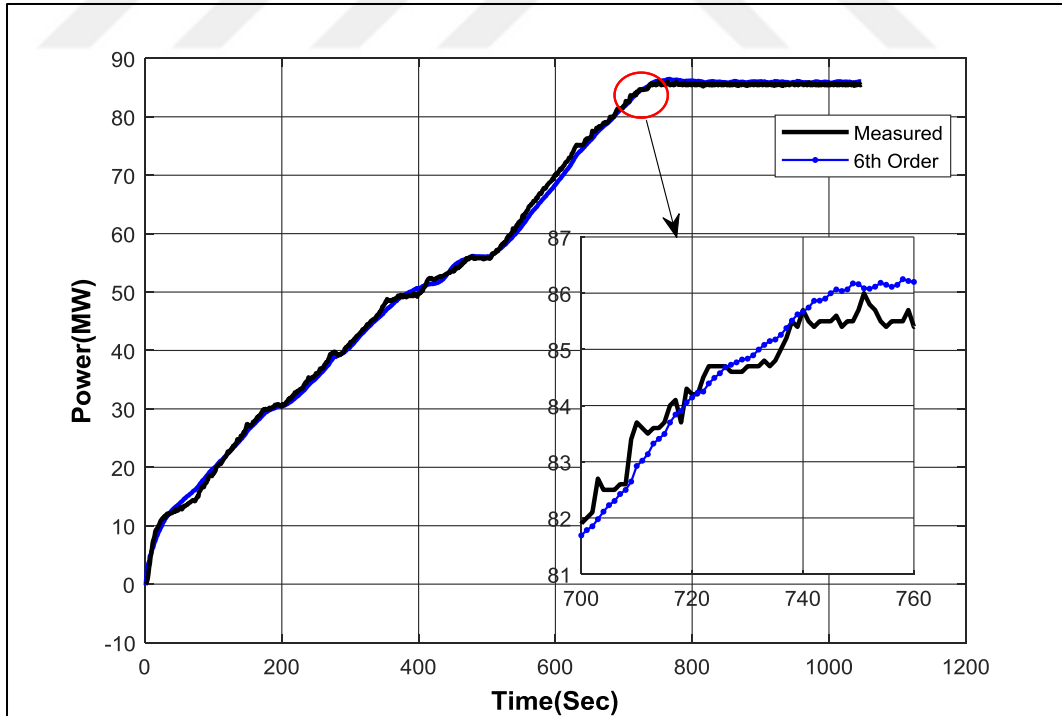


Figure 4.6: 6th Order Comparison Between The State Space Model and The Measurements.

The interpretation of the approximation range of the linear model structure is the error curve over the sampling time with can be shown in Figure 4.7.

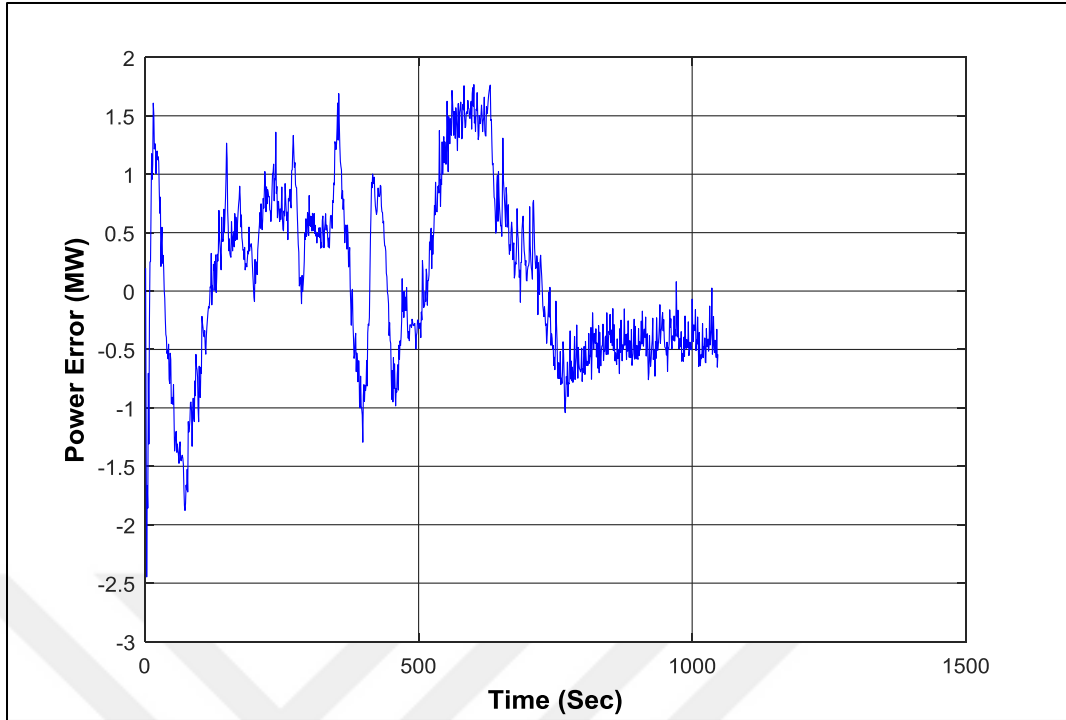


Figure 4.7: Error Curve of Linear Model

4.6.2.2nd order state space model:

The model can be extracted by using the following function:

$$Nt = m(\text{Turbin}, 2nd)$$

Where Nt is the 2nd order discrete-time identified state-space model which is given by:

$$x(t + Ts) = A x(t) + B u(t) + K e(t)$$

$$y(t) = C x(t) + D u(t) + e(t)$$

The state space matrices are :

$$A = \begin{bmatrix} 0.9707 & 0.1993 \\ 0.001675 & 0.8617 \end{bmatrix}$$

$$B = \begin{bmatrix} \text{ExhTemp} & \text{FulePerce} & \text{FuleConsum} & \text{Comp.press.} & \text{Inlet Gid vane} \\ 0.0004622 & 0.005599 & -5.012e-05 & 0.05653 & -0.00109 \\ -5.261e-05 & -0.001677 & -0.005503 & -0.06388 & 0.002002 \end{bmatrix}$$

$$C = [18.58 \quad -1.629]$$

$$D = [0 \quad 0 \quad 0 \quad 0 \quad 0]$$

The Sample time of the measurements is 1 seconds, The Comparison between the state space model and the measurements can be seen in Figure 4.8, and the

evaluation parameters to measure how close the model from the measured data can be described by:

Fit to estimation data: 95.23% (prediction focus)

FPE: 0.03039, MSE: 0.02709

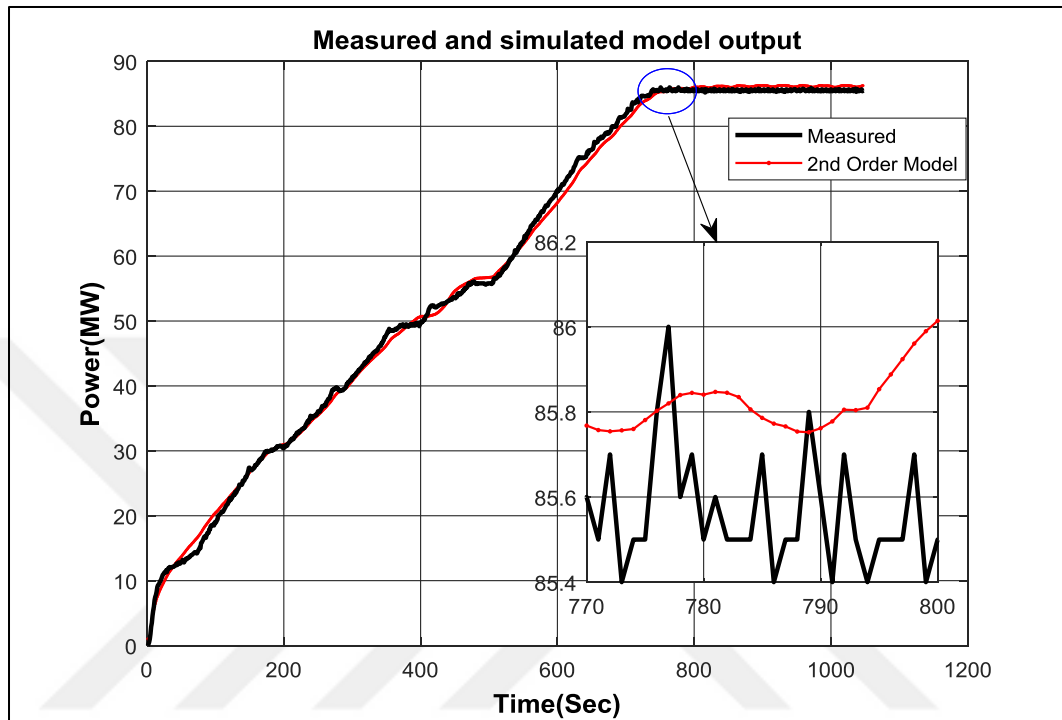
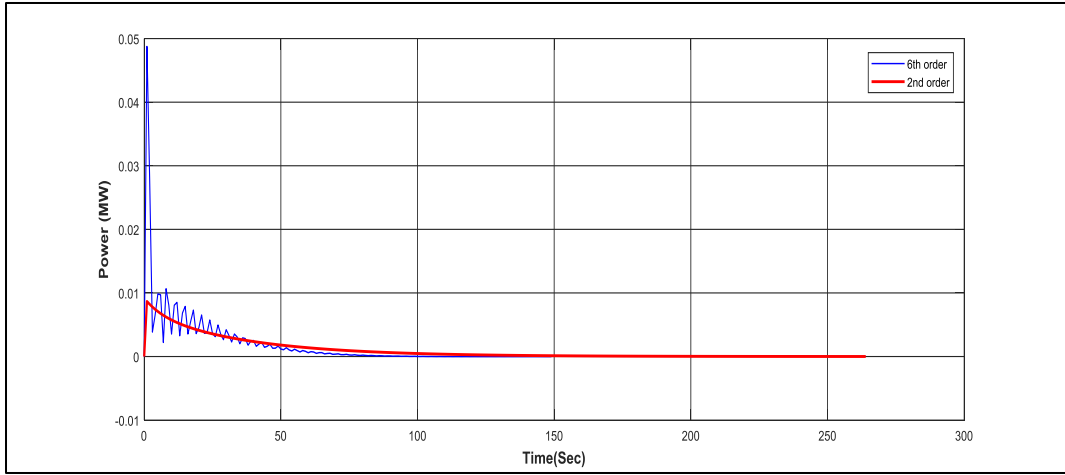


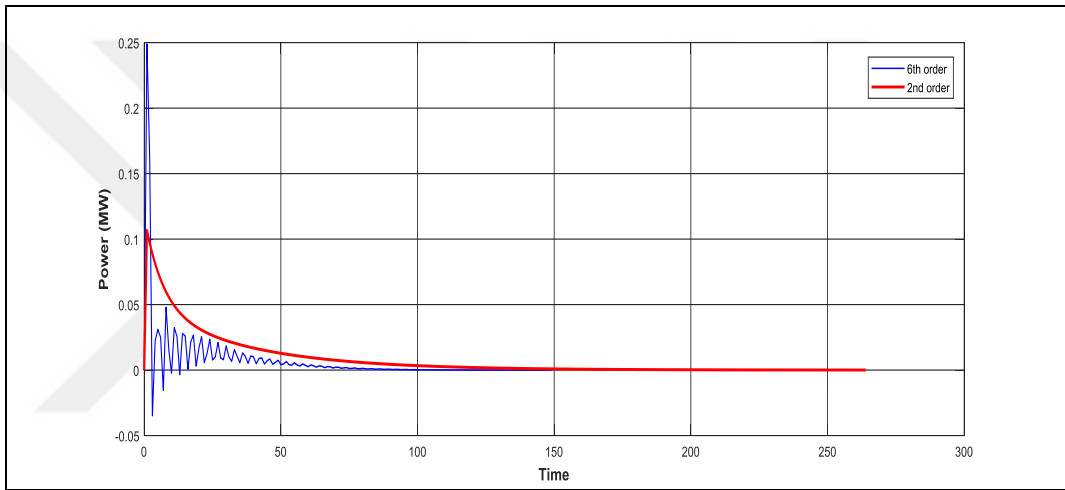
Figure 4.8: 2nd Order Model Comparison Between The State Space Model and The Measurements.

4.6.3. Impulse Responses

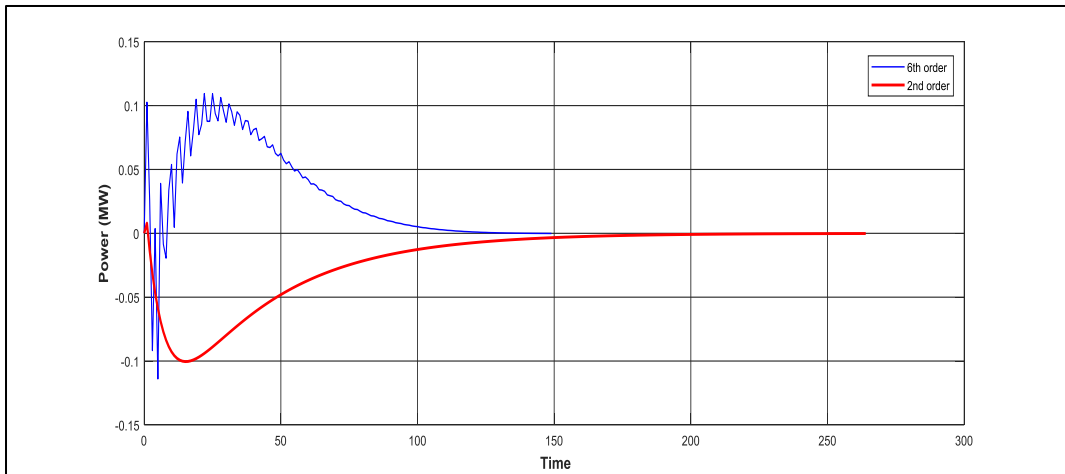
A first step to get a feel for the dynamics is to look at the step responses between the different channels estimated directly from data, Compressor Air Pressure (Cp) in (bar), Exhaust Temp (ET) in (°C), Fule Perce (FP) in (%), Inlet Gide Vane (IGV) in (deg), Fule Consumption (FC) in (kg). The difference between the 6th order and the 2nd when a step and impulse test is applied can be seen in Figure 4.9.



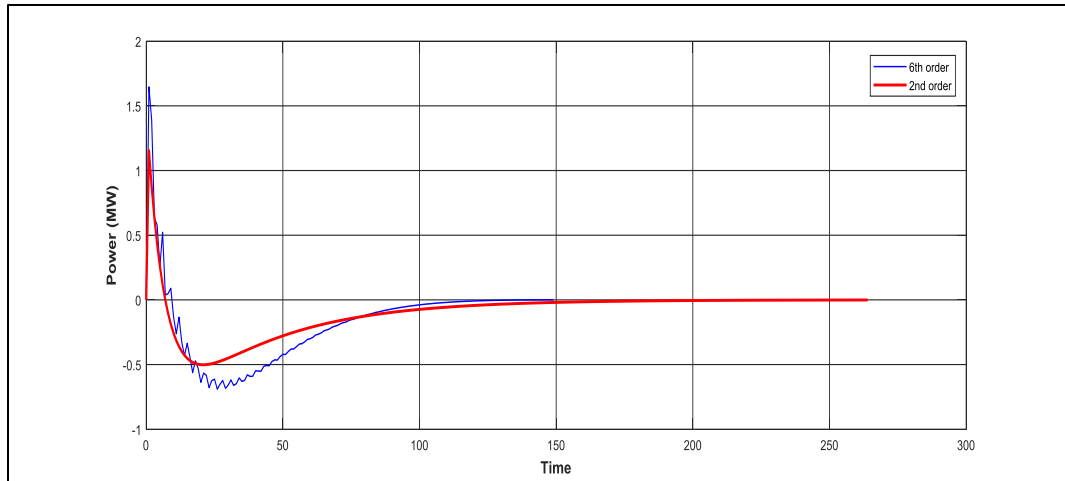
(a)



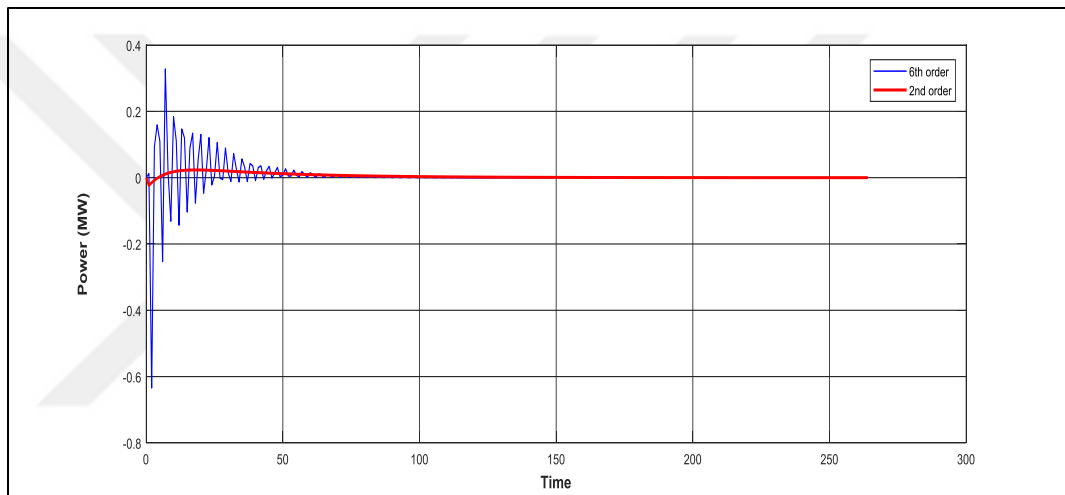
(b)



(c)



(d)



(e)

Figure 4.9: Impulse Responses Comparison for the 2nd & 6th Order Models. Each One Represents The Output Power Response Due to: (a) Exhaust Temperature, (b) Fuel percentage, (c) Fuel Consumption, (d) I G V(e). Compressor Pressure

4.7. Nonlinear Approximations with Nonlinear Descriptions

A Hammerstein model is a specialized model structure where a nonlinear system is approximated by a series connection of a static memory less nonlinear function in series with a linear dynamic plant as shown in Figure 4.10. The Hammerstein model structure is relevant to many engineering applications where nonlinear behavior is the rule rather than the exception [59]. Most physical devices have nonlinear characteristics outside a limited linear range. Control elements, such as valves and position actuators, are typically linear in a limited operating range and possess some form of saturation, hysteresis, or nonlinear characteristics in the input/output characteristic [60].

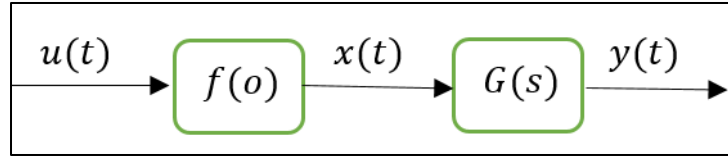


Figure 4.10: Open-Loop Hammerstein System With Static Memory Less Nonlinear Map $F(O)$ and Linear Plant Model G .

In this structure, a nonlinear characteristic of the system is modelled by a static memory less block $f(o)$ and the dynamics of the plant is captured by a linear dynamic model $G(s)$. The internal signal or state $x(t)$ is often unknown or estimated.

Figure 4.11 illustrates the block diagram of a Hammerstein-Wiener model structure. We could study this model as a combination of three series blocks. To formulate the problem, we have an equation (1) which is a nonlinear function transforming input data $u(t)$ and $w(t)$ has the same dimension as $u(t)$.

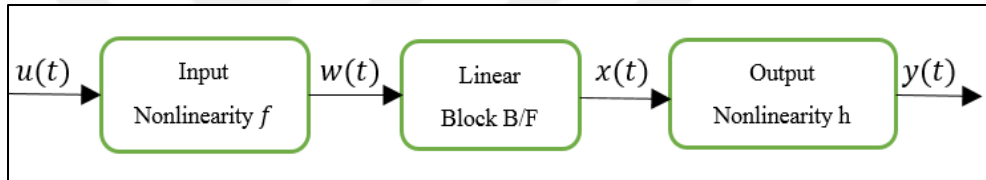


Figure 4.11: Block Diagram of A Hammerstein-Wiener Model

$$\mathbf{w}(t) = \mathbf{f}(\mathbf{u}(t)) \quad (4-14)$$

The second block equation is:

$$\mathbf{x}(t) = \frac{\mathbf{B}}{\mathbf{F}} \mathbf{w}(t). \quad (4-15)$$

Equation (4-13) is a linear transfer function. Has the same dimension as where B and F are similar to polynomials in the linear system model. For outputs and inputs, the linear block is a transfer function (tf) matrix containing entries:

$$tf = \frac{B_{ji}(q)}{F_{ji}(q)} \quad (4-16)$$

Where:

$$\left. \begin{aligned} j &= 1, 2, \dots, n_y \\ i &= 1, 2, \dots, n_u \end{aligned} \right\} \quad (4-17)$$

Finally for the third block:

$$y(t) = h(x(t)) \quad (4-18)$$

Which is a nonlinear function that maps the output of the linear block to the system output. And $x(t)$ are internal variables that define the input and output of the linear block, respectively. Because f acts on the input port of the linear block, this function is called the input nonlinearity. Similarly, because h acts on the output port of the linear block, this function is called the output nonlinearity. If system contains several inputs and outputs, you must define the functions f and h for each input and output signal.

The input-output relationship will be decomposed into two or more interconnected elements, when the output of a system depends nonlinearly on its inputs. So, we can describe the relationship by a linear transfer function and a nonlinear function of inputs. The Hammerstein-Wiener model uses this configuration as a series connection of static nonlinear blocks with a dynamic linear block.

Applications of Hammerstein-Wiener model are in wide areas, for example we can mention modelling electro-mechanical system and radio frequency components, audio and speech processing and predictive control of chemical processes. These models have a useful block representation, transparent relationship to linear systems, and are easier to implement than heavy-duty nonlinear. Therefore, they are very useful. The Hammerstein-Wiener model can be used as a black-box model structure since it prepares a flexible parameterization for nonlinear models. It is possible to estimate a linear model and try to improve its quality by adding an input or output nonlinearity to this model [61]. Also, we can use Hammerstein-Wiener model as a grey box structure to take in physical knowledge about process characteristics. For instance, the input nonlinearity might represent typical physical transformations in actuators and the output nonlinearity might describe common sensor characteristics [62].

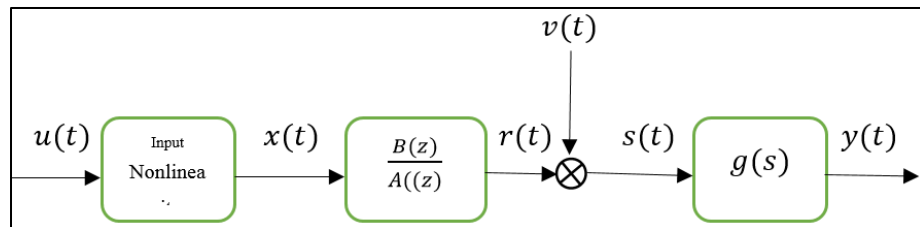


Figure 4.12: (Ha.-w.) Output Error System

The output error system for Hammerstein-Wiener in Figure 4.12 can be expressed as

$$x(t) = f[u(t)] \quad (4-19)$$

$$r(t) = \frac{B(z)}{A(z)}x(t) \quad (4-20)$$

$$s(t) = r(t) + v(t) \quad (4-21)$$

$$y(t) = g[s(t)] \quad (4-22)$$

Where $u(t)$ and $y(t)$ are the system input and output, $x(t), r(t)$ and $s(t)$ are the internal variables, $v(t)$ is stochastic white noise with zero mean, the linear block is an output error model, $A(z)$ and $B(z)$ are polynomials in the unit backward shift operator z^{-1} ($z^{-1}y(t) = y(t-1)$) And defined by

$$A(z) = 1 + a_1z^{-1} + a_2z^{-2} + \dots + a_pz^{-p}$$

$$B(z) = b_1z^{-1} + b_2z^{-2} + \dots + b_qz^{-q}$$

Assume that the orders q and p are known and $y(t) = 0, u(t) = 0$ and $v(t) = 0$ for $t \leq 0$. The input nonlinearity f is modeled as a linear combination of basis functions f_k :

$$x(t) = f[u(t)] = \sum_{k=1}^m c_k f_k[u(t)] \quad (4-23)$$

Where m is the number of the basis functions. The output non-linearity is considered to be invertible, and can be written as a linear combination of the basis functions [63]:

$$s(t) = g^{-1}[y(t)] = \sum_{l=1}^n d_l g_l [y(t)] \quad (4-24)$$

From (4-17), (4-18) and (4-21), we have

$$\begin{aligned} r(t) &= [1 - A(z)]r(t) + B(z)x(t) \\ &= -\sum_{i=1}^p a_i r(t-i) + \sum_{j=1}^q b_j \sum_{k=1}^m c_k f_k[u(t-j)] \end{aligned}$$

Then we have

$$s(t) = -\sum_{i=1}^p a_i r(t-i) + \sum_{j=1}^q b_j \sum_{k=1}^m c_k f_k[u(t-j)] + v(t) \quad (4-25)$$

The objectives of this letter are two-fold: first, by means of the auxiliary model identification idea [64], [65], transform the Hammerstein–Wiener system into a bilinear parameter identification model; second, by means of the hierarchical identification principle [66], [67], present new algorithms to estimate the system parameters (a_i, b_i, c_i, d_i) from available input-output data $y(t), u(t)$.

Notice that parameters in (4-22) and (4-23) are not unique. Without loss of generality, assume that the first coefficient of the non-linear part is unity, i.e., $d_1 = 1$ [68]. Combining (4-22) and (4-23) gives

$$g_1[y(t)] = -\sum_{i=1}^n d_i g_1[y(t)] - \sum_{i=1}^p a_i r(t-i) + \sum_{j=1}^q b_j \sum_{k=1}^m c_k f_k[u(t-j)] + v(t) \quad (4-26)$$

4.8. Results (Nonlinear Model)

Many practical applications, such as the fuel control of a gas turbine engine, can be modelled by a feedback connection of a linear controller in series with a Hammerstein system, where the nonlinearity provides a representation of the control element or actuator. An iterative gradient-based method is proposed to simultaneously identify the nonlinear fuel valve characteristic and a low-order linear plant model in gas turbine applications that leverages a priori knowledge of both the nonlinearity and engine dynamics. The identification is a nonlinear prediction error minimization method in a closed loop

The model where a nonlinear block both precedes and follows a linear dynamic system is called a Hammerstein-Wiener model. This is illustrated diagrammatically in Figure 4.13.

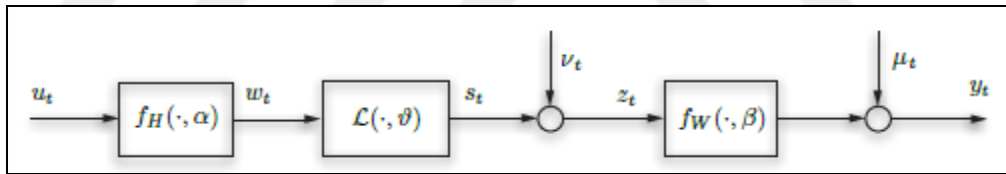


Figure 4.13 The General Hammerstein-Wiener Model Structure, Which Consists of Sandwiching A Linear Time Invariant System L Between Memory Less Nonlinearities f_H and f_W .

The same condition and number of inputs for the linear system modelling. Hammerstein-Wiener model here applied with 1 output and 5 inputs.

At 1(sec) Sampling interval several trails by adopting the system identification, the linear transfer function matrix corresponding parameters can be given by the variables nb , nf and nk :

$$nb = [2 \ 2 \ 2 \ 2 \ 2], \quad nf = [3 \ 3 \ 3 \ 3 \ 3], \quad nk = [1 \ 1 \ 1 \ 1 \ 1]$$

Where:

nb : is the number of zeros.

nf : is the number of poles.

nk : is the input delay.

The nonlinearity estimators selected for each input as: For input 1, 2, 3, 4, and 5: pw linear with 10 units

The output nonlinearity estimator is also pw linear with 10 units, the loss function: 0.027864 to get a Best fit of a 99.35 % as shown in Figure 4.14 the general Hammerstein-Wiener model structure

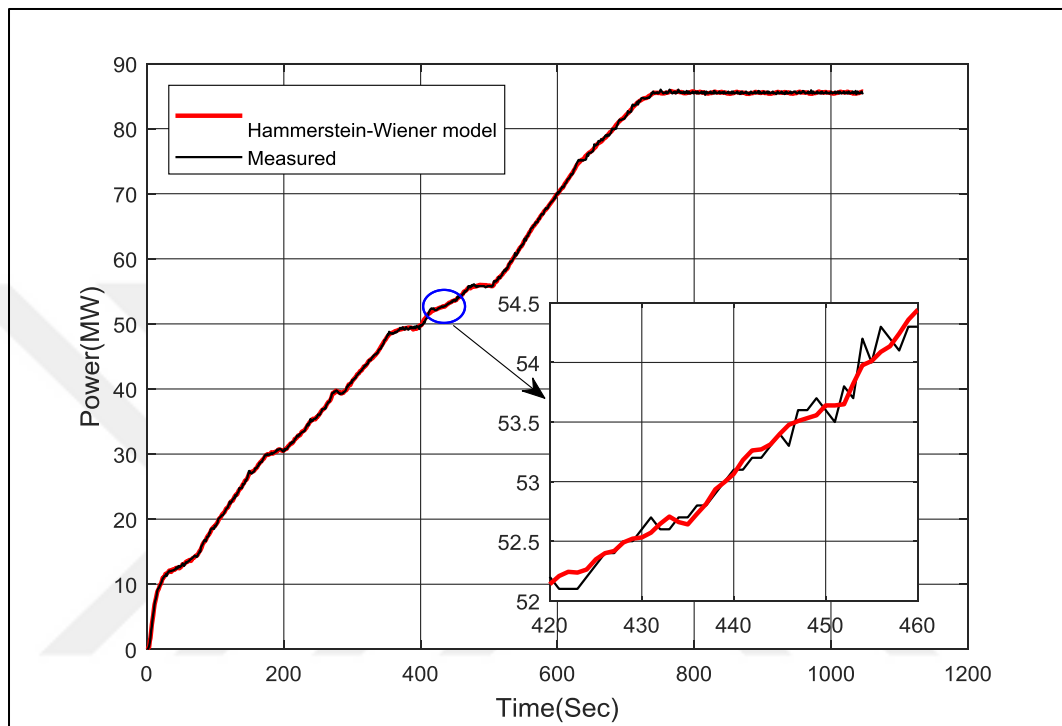


Figure 4.14: The General Hammerstein-Wiener Model Structure, Which Consists Of

To declare the difference between the linear and nonlinear model along with the observations, Figure 4.15.

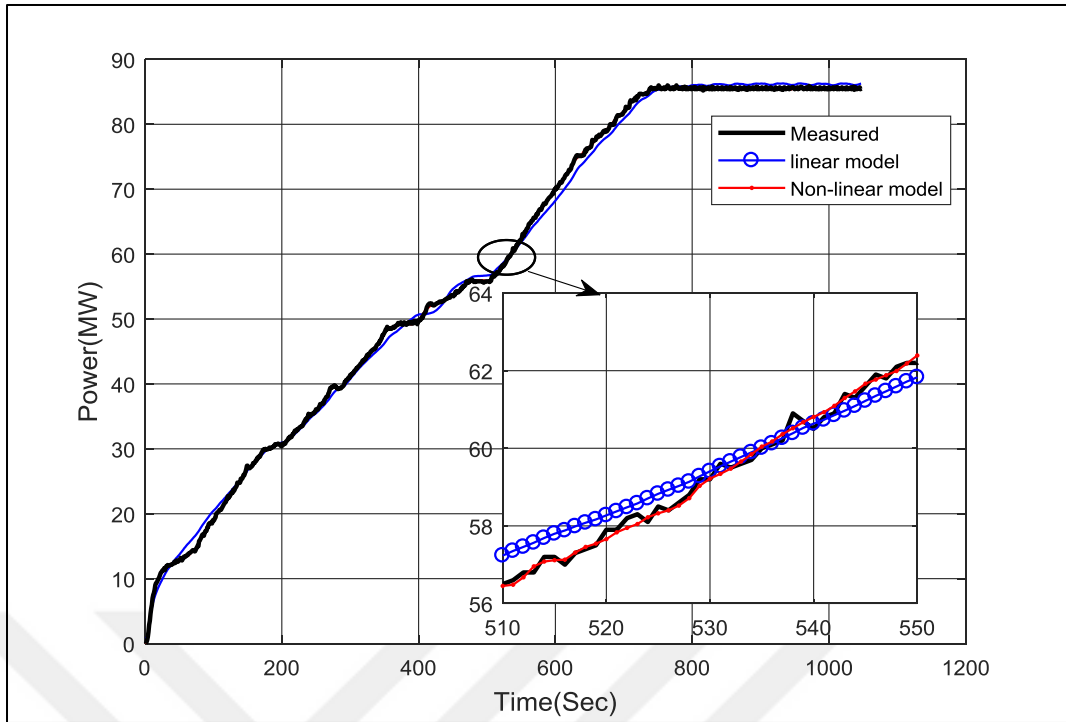


Figure 4.15: Linear, Non-Linear Models and The Field Measurements

To declare the fitting approximation of both proposed linear and non-linear models, a comparison of those two models have been drawn as compared with filed measurements, as can be seen in Figure 4.16.

Another interpretation of the approximation range of the Hammerstein-Wiener model structure is the error curve over the sampling time with can be shown in Figure 4.17.

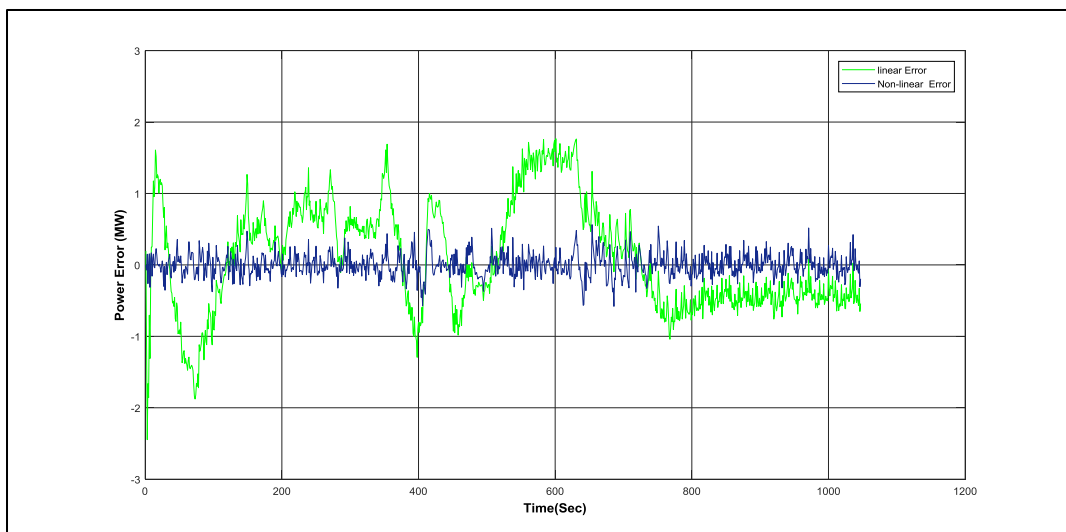


Figure 4.16: Linear, Non-linear models and the field measurements (zoom in)

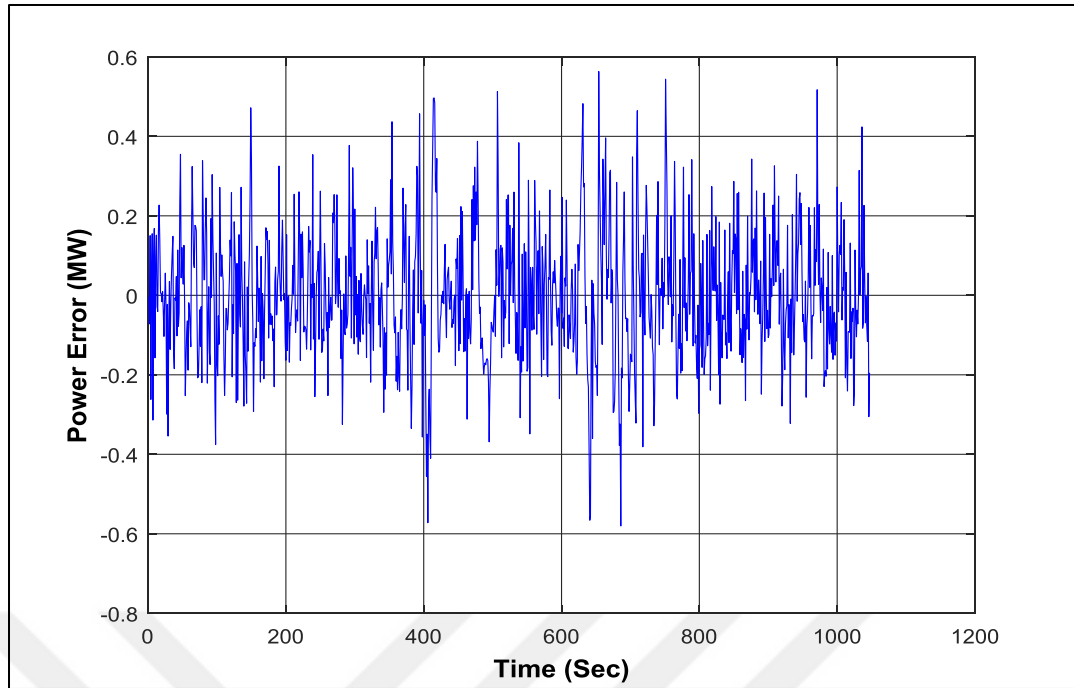


Figure 4.17: Error Curve of Non-Linear (Hammerstein) Model

To declare the difference between (Non-linear (Hammerstein), and linear(2nd order and 6th order),ANN) models a comparison of those two models have been drawn as compared with filed measurements, as can be seen in Figure 4.18.

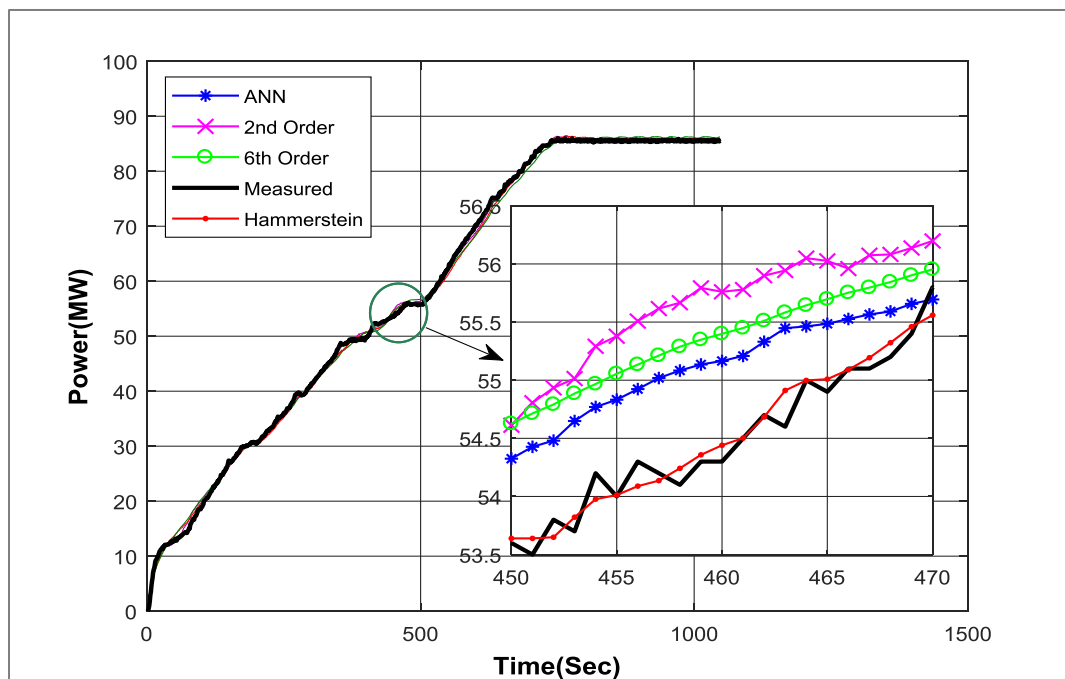


Figure 4.18: Linear, Non-Linear, ANN Models and The Field Measurements

To compare the approximation that Hammerstein-Wiener model provides with the linear model and custom ANN model, the error curve over the sampling time for all of them with respect to power observations can be shown in Figure 4.19.

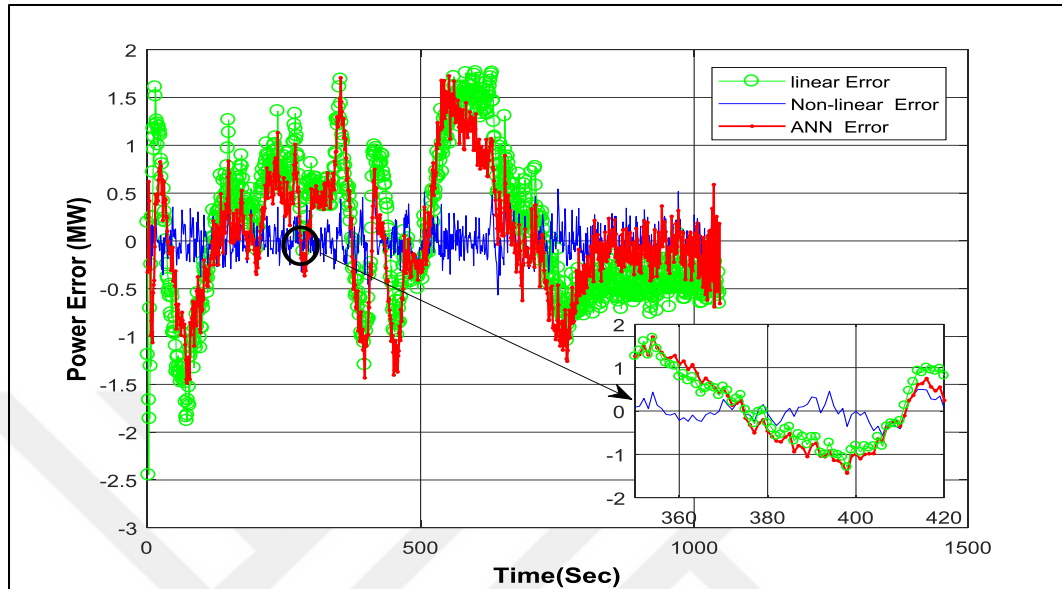


Figure 4.19: Comparison Between Error Curves Due to The Non-Linear [Hammerstein, Ann] Model and The Linear Model.

CHAPTER FIVE

CONCLUSIONS AND RECOMMENDATION

5.1. CONCLUSIONS

There are different approaches and methodologies in modelling and control of gas turbines. Choosing the right method and creating the right model based on the required application depends on different factors. A short description of each of these factors, including GT type, GT configuration, modelling methods, modelling objectives as well as control system type and configuration were provided. Samples of significant research related to each of the areas were presented. By highlighting the mentioned factors, remarkable enhancements can be achieved in the process of modelling and control of gas turbines.

Modelling and control of gas turbines (GTs) have always been a controversial issue because of the complex dynamics of these kinds of equipment. Considerable research activities have been carried out so far in this field in order to disclose the secrets behind the nonlinear behaviour of these systems. Although the results of the research in this area have been satisfactory so far, it seems that there is no end to the efforts for performance optimization of gas turbines. A variety of analytical and experimental models as well as control systems have been built so far for gas turbines. However, the need for optimized models for different objectives and applications has been a strong motivation for researchers to continue to work in this field.

The assessment of the applied method evaluated by the fitting percentage to estimate the experimental data and the Mean Square Error (MSE). The challenges faced when a practical field measurements have been adopted for the gas turbine model GE Frame 9E of the Alquds-Iraq power plant as a multi-input case study. Firstly, data analysis has been applied to classify the input-input and input-output relationships for reducing the number of inputs.

A linear model has been addressed initially with the most effective parameters represented by the Fuel Consumption (FC) and Exhaust Temperature (ET), has been evaluated for the measurements of the system to attain some preliminary insight into the data characteristics.

Considerable research activities have been carried out so far in this field in order to disclose the secrets behind the nonlinear behaviour of these systems. Although the results of the research in this area have been satisfactory so far, it seems that there is no end to the efforts for performance optimization of gas turbines. A variety of analytical and experimental models as well as control systems have been built for gas turbines. A reasonable results with significant fitting for the field measurements has been attained from adopting approaches and can be briefly listed as in the Table 5.1.

Table 5.1: A comparison of the models under study.

Description	Custom ANN	Linear TF model	State-space Estimation model	Non-linear Hammerstein
Complexity	Simple	Intermediate	Intermediate	Complex
Providing mathematical formula	Provides a formula represents the output power of the system	Transfer function as a black box 2 nd Order	State space model 6 th Order	Several mathematical expressions
Facility for further analysis	Difficult	Easy	Easy	Intermediate
Approximation accuracy	Higher for high number of hidden neurons and layers	Higher in high order	Proportional with number of state variables	Equivalent to the nonlinearity portions of the outcome equations
Best fit percentage	97.39%	96.43%	97 %	99.35

5.2. Recommendations

The extraction of the mathematical modelling equation for the gas turbine (Model: Frame 9) system in power plant application, is possible if it is taken into account the availability of the field-based experimental data for all the effected inputs

to the generated output power. As a continuation of the work conducted for this thesis, suggestions for future research include the following:

1. Expanding the application of this proposed algorithm and procedure in the power plant systems that based on the gas turbine to drive its generators.
2. Utilizing the significant contribution outcome of this study, which represented by the single mathematical model equation based on custom ANN for further investigations and control purposes.
3. Since the research outcomes provide thorough mathematical model comparisons that used the previous recorded measurements, they can be used to estimate the future behaviour of the system.
4. For more precise mathematical representation of the output generated power of such systems, several operation conditions are needed in adequate numbers of cycles over the time.
5. Applying mathematical modelling for such dynamic systems to estimate the performance or controlling some adaptive processes to be an economical and time saving solution for large scale power plant applications.

Implementing the proposed modeling method to investigate and modelling of subsystems individually in a more detailed as well as utilizing the same modeling results to simulate the system with its equivalent passive and active elements.

REFERENCES

- [1] A. K. S. Jardine, D. Lin, and D. Banjevic, "A review on machinery diagnostics and prognostics implementing condition-based maintenance," *Mechanical Systems and Signal Processing*, vol. 20, no. 7, pp. 1483–1510, 2006.
- [2] M. Pecht, "Prognostics and health management of electronics," no. Wiley Online Library., 2008.
- [3] D. Galar, U. Kumar, J. Lee, and W. Zhao, "Remaining Useful Life Estimation using Time Trajectory Tracking and Support Vector Machines," *J. Phys. Conf. Ser.*, vol. 364, p. 12063, 2012.
- [4] X. S. Si, W. Wang, C. H. Hu, and D. H. Zhou, "Remaining useful life estimation - A review on the statistical data driven approaches," *Eur. J. Oper. Res.*, vol. 213, no. 1, pp. 1–14, 2011.
- [5] A. Heng, S. Zhang, A. C. C. Tan, and J. Mathew, "Rotating machinery prognostics: State of the art, challenges and opportunities," *Mechanical Systems and Signal Processing*, vol. 23, no. 3, pp. 724–739, 2009.
- [6] A. Lazzaretto and A. Toffolo, "Analytical and neural network models for gas turbine design and off-design simulation," *Int. J. Appl. Thermodyn.*, vol. 4, no. 4, pp. 173–182, 2001.
- [7] S. O. T. Ogaji, R. Singh, and S. D. Probert, "Multiple-sensor fault-diagnoses for a 2-shaft stationary gas-turbine," *Appl. Energy*, vol. 71, no. 4, pp. 321–339, 2002.
- [8] A. L. Jaime ARRIAGADA, "Magnus GENRUP" and M. ASSADI, "Fault Diagnosis System for an Industrial Gas Turbine by Means of Neural Networks," *Proc. Int. Gas Turbine Congr. 2003 Tokyo Novemb. 2-7, 2003*, 2003.
- [9] M. Basso, L. Giarré, S. Groppi, and G. Zappa, "NARX models of an industrial power plant gas turbine," *IEEE Trans. Control Syst. Technol.*, vol. 13, no. 4, pp. 599–604, 2005.

- [10] R. Bettocchi, P. R. Spina, M. Pinelli, M. Venturini, and M. Burgio, "Set up of a robust neural network for gas turbine simulation," in Proceedings of the ASME Turbo Expo 2004, 2004, vol. 4.
- [11] R. Bettocchi, P. R. Spina, M. Pinelli, and M. Venturini, "Artificial intelligence for the diagnostics of gas turbines. Part I: Neural network approach," in Proceedings of the ASME Turbo Expo, 2005, vol. 4.
- [12] F. Jurado, "Non-linear modeling of micro-turbines using NARX structures on the distribution feeder," *Energy Convers. Manag.*, vol. 46, no. 3, pp. 385–401, 2005.
- [13] NG CHOO GEON, "USING ARTIFICIAL NEURAL NETWORK TO PREDICT POWER PLANT TURBINE HALL KEY COST DRIVERS," *Fac. Civ. Eng. Univ. Teknol. Malaysia*, 2007.
- [14] P. R. Spina and M. Venturini, "Gas turbine modeling by using neural networks trained on field operating data," in ECOS 2007 - Proceedings of the 20th International Conference on Efficiency, Cost, Optimization, Simulation and Environmental Impact of Energy Systems, 2007, vol. 1.
- [15] T. Palmé, M. Fast, M. Assadi, A. Pike, and P. Breuhaus, "Different Condition Monitoring Models for Gas Turbines by Means of Artificial Neural Networks," in ASME Turbo Expo 2009, 2009, pp. 543–553.
- [16] M. Fast, M. Assadi, and S. De, "Development and multi-utility of an ANN model for an industrial gas turbine," *Appl. Energy*, vol. 86, no. 1, pp. 9–17, 2009.
- [17] T. Palmé, M. Fast, and M. Thern, "Gas turbine sensor validation through classification with artificial neural networks," *Appl. Energy*, vol. 88, no. 11, pp. 3898–3904, 2011.
- [18] M. Fast and T. Palmé, "Application of artificial neural networks to the condition monitoring and diagnosis of a combined heat and power plant," *ECOS 2008 21st Int. Conf. Effic. Cost, Optim. Simul. Environ. Impact Energy Syst.*, vol. 35, no. 2, pp. 1114–1120, 2010.
- [19] M. Fast and T. Palmé, "Application of artificial neural networks to the condition monitoring and diagnosis of a combined heat and power plant," *Energy*, vol. 35, no. 2, pp. 1114–1120, 2010.
- [20] Y. Yoru, T. H. Karakoc, and a. Hepbasli, "Application of Artificial Neural Network (ANN) Method to Exergy Analysis of Thermodynamic Systems," 2009 Int. Conf. Mach. Learn. Appl., 2009.

- [21] C. M. Bartolini, F. Caresana, G. Comodi, L. Pelagalli, M. Renzi, and S. Vagni, "Application of artificial neural networks to micro gas turbines," *Energy Convers. Manag.*, vol. 52, no. 1, pp. 781–788, 2011.
- [22] K. Levenberg and K. Levenberg, "A Method for the Solution of Certain Problems in Least Squares," in *Quart. Appl. Math.*, 1944, vol. 2, no. 2, pp. 164--168.
- [23] and W. T. V. W. H. Press, B. P. Flannery, S. A. Teukolsky, "Numerical Recipes in C," Cambridge, MA Cambridge Univ. Press, 1988.
- [24] G. Lera and M. Pinzolas, "A quasi-local Levenberg-Marquardt algorithm for neural network training," *Neural Networks Proceedings*, 1998. *IEEE World Congr. Comput. Intell. 1998 IEEE Int. Jt. Conf.*, vol. 3, pp. 2242–2246 vol.3, 1998.
- [25] J. Dongarra et al., "LINPACK User's Guide," Philadelphia, PA SIAM, 1979.
- [26] M. Schwabacher and K. Goebel, "A survey of artificial intelligence for prognostics," *Assoc. Adv. Artif. Intell. AAAI Fall Symp.* 2007, pp. 107–114, 2007.
- [27] C. S. Byington, M. Watson, and D. Edwards, "Data-driven neural network methodology to remaining life predictions for aircraft actuator components," in *IEEE Aerospace Conference Proceedings*, 2004, vol. 6, pp. 3581–3589.
- [28] W. S. Sarle, "Neural Networks and Statistical Models," *SAS USers Gr. Int. Conf.*, p. 13, 1994.
- [29] N. Murata, S. Yoshizawa, and S. Amari, "Network information criterion - determining the number of hidden units for an artificial neural network model," *IEEE Trans. Neural Networks*, vol. 5, no. 6, pp. 865–872, 1994.
- [30] S. Haykin and X. B. Li, "Detection of Signals in Chaos," *Proc. IEEE*, vol. 83, no. 1, pp. 95–122, 1995.
- [31] S. Haykin and J. Principe, "Making sense of a complex world [chaotic events modeling]," *IEEE Signal Process. Mag.*, vol. 15, no. 3, pp. 66–81, 1998.
- [32] J. M. P. Menezes and G. A. Barreto, "Long-term time series prediction with the NARX network: An empirical evaluation," in *Neurocomputing*, 2008, vol. 71, no. 16–18, pp. 3335–3343.
- [33] A. Sorjamaa, J. Hao, N. Reyhani, Y. Ji, and A. Lendasse, "Methodology for long-term prediction of time series," *Neurocomputing*, vol. 70, no. 16–18, pp. 2861–2869, 2007.

- [34] A. Saxena, K. Goebel, D. Simon, and N. Eklund, "Damage propagation modeling for aircraft engine run-to-failure simulation," in 2008 International Conference on Prognostics and Health Management, PHM 2008, 2008.
- [35] E. Bai, "A blind approach to the Hammerstein – Wiener model identification," *Automatica*, vol. 38, pp. 967–979, 2002.
- [36] L. Ljung, "System Identification: Theory for the Users, 2nd ed. Upper Saddle River," no. Prentice-Hall, 1999.
- [37] and H. I. H. S.] H. Cohen, G.F.C. Rogers, "Gas turbine theory. 3rd ed," no. Longman, 1987.
- [38] A. J. Fawke, H. I. H. Saravanamuttoo, and M. Holmes, "Experimental Verification of a Digital Computer Simulation Method for Predicting Gas Turbine Dynamic Behaviour," *Proc. Inst. Mech. Eng.*, vol. 186, no. 1, pp. 323–329, 1972.
- [39] T. Shobeiri, "Digital computer simulation of the dynamic operating behaviour of gas turbines," no. Brown Boveri Review, 1987.
- [40] A. Hussain and H. Seifi, "Dynamic modeling of a single shaft gas turbine," in IFAC Symposia Series, 1992, no. 9.
- [41] W. W. Hung, "Dynamic Simulation of Gas-Turbine Generating Unit," *IEE Proc. C Gener. Transm. Distrib.*, vol. 138, no. 4, p. 342, 1991.
- [42] W. I. Rowen, "Simplified Mathematical Representations of Heavy-Duty Gas Turbines," *J. Eng. Power*, vol. 105, no. 83, p. 865, 1983.
- [43] M. Rahnama, H. Ghorbani, and A. Montazeri, "Nonlinear identification of a gas turbine system in transient operation mode using neural network," in 4th Conference on Thermal Power Plants, CTPP 2012, 2012.
- [44] C. Jin, P. Wang, J. Xiao, and S. Member, "Implementation of Hierarchical Control in DC Microgrids," vol. 61, no. 8, pp. 4032–4042, 2014.
- [45] N. Chiras, C. Evans, and D. Rees, "Global Nonlinear Modeling of Gas Turbine Dynamics Using NARMAX Structures," *J. Eng. Gas Turbines Power*, vol. 124, no. 4, p. 817, 2002.
- [46] I. Yousefi, H. Khaloozadeh, and A. M. Ali, "Identification and fault diagnosis of an industrial gas turbine using State-Space methods," *Advanced Materials Research*, vol. 383–390. pp. 1000–1006, 2012.
- [47] R. T. Meyer, R. A. DeCarlo, S. Pekarek, and C. Doktorcik, "Gas Turbine Engine Behavioral Modeling," *J. Eng. Gas Turbines Power*, vol. 137, no. 12, p. 122607, 2015.

- [48] D. Olivenza-León, A. Medina, and A. Calvo Hernández, “Thermodynamic modeling of a hybrid solar gas-turbine power plant,” *Energy Convers. Manag.*, vol. 93, pp. 435–447, 2015.
- [49] M. P. Boyce, *Gas Turbine Engineering Handbook*. 2012.
- [50] V. T. Chand, B. R. Sankar, and J. R. Chowdary, “Exergy Analysis of Gas Turbine Power Plant,” *Int. J. Eng. Trends Technol.*, vol. 4, no. 9, pp. 3991–3993, 2013.
- [51] M. Mostafavi, a. Alaktwi, and B. Agnew, “Thermodynamic analysis of combined open-cycle-twin-shaft gas turbine (Brayton cycle) and exhaust gas operated absorption refrigeration unit,” *Appl. Therm. Eng.*, vol. 18, pp. 847–856, 1998.
- [52] L. N. Hannett, G. Jee, and B. Fardanesh, “A governor/turbine model for a twin-shaft combustion turbine,” *IEEE Trans. Power Syst.*, vol. 10, no. 1, pp. 133–140, 1995.
- [53] Y. S. H. Najjar, “Comparison of performance for cogeneration systems using single- or twin-shaft gas turbine engines,” *Appl. Therm. Eng.*, vol. 17, no. 2, pp. 113–124, 1997.
- [54] R. T. Harman, “Gas Turbine Engineering: Applications, Cycles and Characteristics”.
- [55] P. Breeze, *Gas-Turbine Power Generation*. 2016.
- [56] K. Jordal, “Modeling and performance of gas turbine cycles with various means of blade Cooling,” Lund, Sweden, 2001.
- [57] J. C. Wang, H. D. Chiang, Y. T. Chen, C. L. Chang, C. Y. Huang, and C. T. Huang, “Identification of Excitation System Models Based on On-line Digital Measurements,” *IEEE Trans. Power Syst.*, vol. 10, no. 3, pp. 1286–1293, 1995.
- [58] Joseph W. Comish, “Test guidelines for synchronous unit dynamic testing and model validation. WSCC control group and modeling & validation work group,” 1997.
- [59] E. W. Bai, “Identification of linear systems with hard input nonlinearities of known structure,” in *IFAC Proceedings Volumes (IFAC-PapersOnline)*, 2002, vol. 15, no. 1, pp. 97–102.
- [60] Y. Han and R. A. De Callafon, “Closed-loop identification of Hammerstein systems using iterative instrumental variables,” in *IFAC Proceedings*

Volumes (IFAC-PapersOnline), 2011, vol. 18, no. PART 1, pp. 13930–13935.

- [61] J. W. Van Wingerden and M. Verhaegen, “Closed-loop subspace identification of Hammerstein-Wiener models,” in Proceedings of the IEEE Conference on Decision and Control, 2009, pp. 3637–3642.
- [62] D. Wang and S. X. Chen, “Empirical likelihood for estimating equations with missing values,” *Ann. Stat.*, vol. 37, no. 1, pp. 490–517, 2009.
- [63] E. W. Bai, “An optimal two stage identification algorithm for Hammerstein-Wiener nonlinear systems,” in Proceedings of the American Control Conference, 1998, vol. 5, pp. 2756–2760.
- [64] F. Ding, G. Liu, and X. P. Liu, “Parameter estimation with scarce measurements,” *Automatica*, vol. 47, no. 8, pp. 1646–1655, 2011.
- [65] D. Q. Wang, “Least squares-based recursive and iterative estimation for output error moving average systems using data filtering,” *IET Control Theory Appl.*, vol. 5, no. 14, pp. 1648–1657, 2011.
- [66] F. Ding and T. Chen, “Hierarchical least squares identification methods for multivariable systems,” *IEEE Trans. Automat. Contr.*, vol. 50, no. 3, pp. 397–402, 2005.
- [67] Z. Zhang, F. Ding, and X. Liu, “Hierarchical gradient based iterative parameter estimation algorithm for multivariable output error moving average systems,” *Comput. Math. with Appl.*, vol. 61, no. 3, pp. 672–682, 2011.
- [68] D. Wang and F. Ding, “Extended stochastic gradient identification algorithms for Hammerstein-Wiener ARMAX systems,” *Comput. Math. with Appl.*, vol. 56, no. 12, pp. 3157–3164, 2008.